CANATEC Associates International Ltd.

FEED Services, Field Operations Support
Instruments, Software, Training

Tracking Ice Islands and Multi-Year Hummock Fields from Ellesmere Island to the Chukchi Sea

Final Report

October, 2011

Dr. Scott Tiffin, Tyler Sylvestre, Doug Hagen, Dr. Roger Pilkington, Dr. Ian Turnbull

SUMMARY

This is the fourth and final analysis of tracking data and imagery for the JIP. It covers the period from beginning of November 2010 to end of June 2011, and summarizes the data for the entire period in which the beacons were active, from mid-May 2009 to the end of June 2011. The format of the analysis in this report is identical to the previous one in terms of drift, description of visual features and area/shape changes, with the addition of a section summarizing the whole project results. As of the end of June 2011, only the beacon on Ice Island 7E remained transmitting and within the area of interest to this project. This very large feature moved SW and then west through the southern Beaufort Sea, with an intermittent beacon that appears now to have failed, so this feature can no longer be easily tracked. The project has generated very important original data on ice island and multiyear hummock fields that can help create initial parameters for hazard management in operations and for design criteria for structures. However, the data are so few that more studies of the same phenomena are required.

Alastair Ross Technology Centre
#122, 3553 – 31st Street N.W., Calgary, Alberta, Canada T2L 2K7
(403) 228-0962; fax (403) 282-1238; www.canatec.ca

TABLE OF CONTENTS

List of Figures

List of Tables

1 BACKGROUND

This is the fourth and final in a series of analytical reports being written over the two-year duration of this project. All reports follow a similar format, reporting on the conditions during the time frame covered by the report. However, there is a change in emphasis in each report: the first focused on image techniques; the second emphasized area and shape changes; and the third was a demonstration of the utility of the concepts and techniques for analysis of clustering and dispersion of ice fragments around an ice island, for future application. This fourth report focuses on the final analysis period of November 2010 to June 2011, and then summarizes the drift data for the entire two-year period from May 2009 to June 2011

2 OBJECTIVES OF THIS REPORT

The objectives of the present report are to provide an analysis of the ice islands and multiyear hummock fields (MYHFs) being tracked during the period of beginning November 2010 to end June 2011. The report also summarizes the data obtained over the entire two-year beacon drift period, their: drift patterns and velocities; and their patterns of growth and decay.

3 DATA

3.1 Beacon Data Streams

Figure 3-1 shows the periods when the 2 functioning beacons were operating for the period from November 1, 2010 through June 30, 2011. Gaps in the transmissions are presumably due to snow or water accumulation over the beacon or caused by electronic problems. We suspect beacon 7E transmission difficulties continue to be electronic, as this same erratic pattern has continued practically since it was deployed. The beacon on 7E was working intermittently as of June 30, 2011, but has since died.

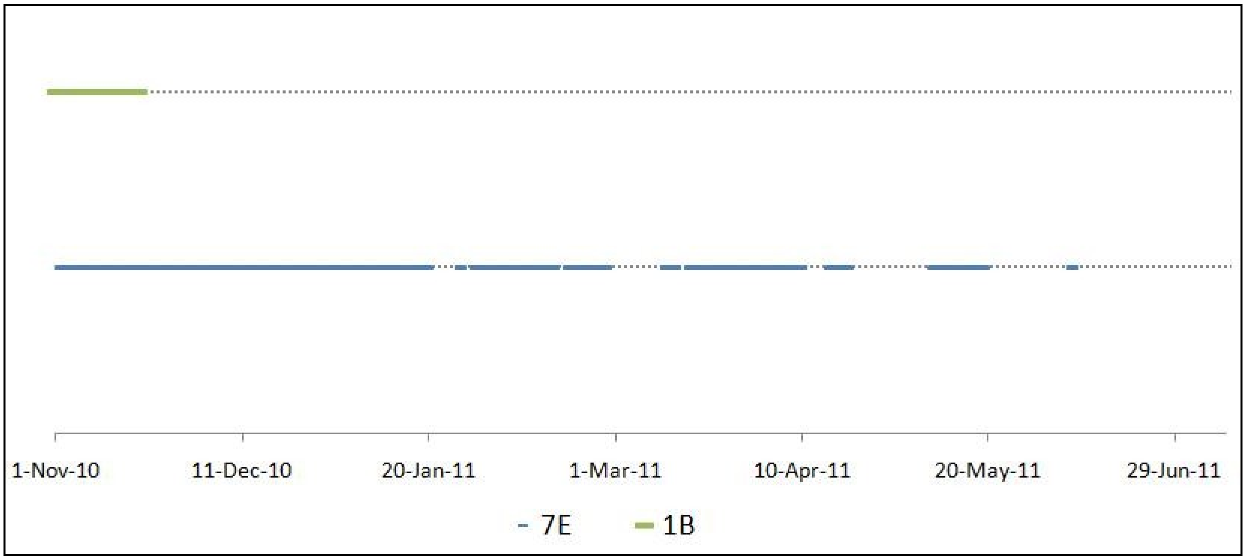

Figure 3-1: Solid Lines indicate when Beacons were Operating

As will be shown in the next chapter, Ice Island 7E is our most important Target, so extracting as much data from the erratic beacon as possible was considered a high priority.

3.2 Image Acquisition

In order to satisfy the objective to better understand patterns of growth and decay of our features, high resolution satellite images are needed. We obtained both Fine-Quad and Fine images for Target 7E. Table 3-1 provides a summary of the set of images which were acquired via RadarSat-2 satellite over our reporting period.

Table 3-1: Summary of Image Acquisitions.

Target Name	Image Acquisition Date	Beam Mode	Resolution
7E	11/04/2011	Fine Quad (HV polarization)	12 m
	15/05/2011	Fine (dual polarization (VV, VH))	8 m

Only two images could be obtained for 7E on account of significant intermittent transmission not allowing us to specify the image taking location. No images were acquired for Target 1B because image collection was to resume in April 2011 but the beacon on Target 1B stopped transmitting on November 17, 2010.

3.3 Website Data Displays

Access to the Canatec website is found at www.canatec.ca. The clients can access the beacon tracks by clicking on the Tracking Beacon button, then entering the confidential UserID and passwords already supplied to them. Since the last report we have new graphs to automatically show latitude, longitude, speed in cm/s, and direction in degrees, all as a function of time for each target. This report has more detail on certain aspects of movement, but the advantage of the website is that partners can select specific portions of the tracks and get outputs automatically as they require. All track data can be loaded down, so that clients can plot and/or perform their own analyses on the data.

4 DRIFT ANALYSIS

4.1 General Situation

Figure 4-1 shows the drift of all targets between November 1, 2010 and June 30, 2011. In the following sections, we describe the movement of the beacons on Targets 7E and 1B separately and analyze the patterns and statistical properties of each trajectory over this time period. All other targets had either left the region of interest or had dead beacons by November 1, 2010. It should be noted that only positions approximately every 24 hours are used in this analysis in order to filter out spurious data, however, all drift speeds are converted into km/day. In addition, positions were re-sampled to about every 24 hours for all targets because we are concerned with daily position changes. We do not have the meteorological and oceanographic data to rigorously analyze higher-frequency ice motion.

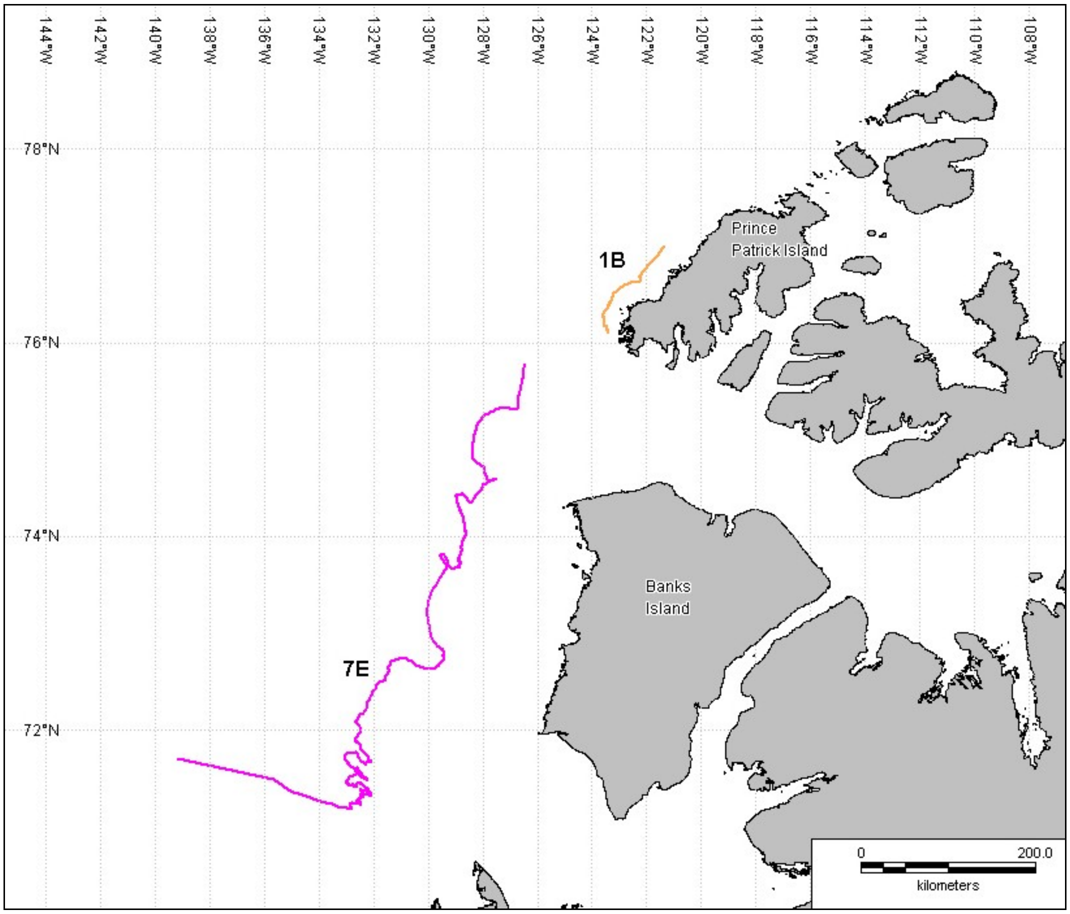

Figure 4-1: Drift of the ice beacons from November 1, 2010 to June 30, 2011.

4.1.1 Target 7E

Figure 4-2 shows that during the time period November 1, 2010 to June 30, 2011 Target 7E continued its general southwest drift from the previous analyses, moving from approximately 76°N to 71.7°N. Numerous exceptions to the general southwest drift are observed, however, with the target drifting in a direction other than the southwest for 68% of the November-June period. In parts of every month from early November through about May 2, frequent excursions to the east-southeast and northwest are observed, with subsequent excursions to the west-southwest. Throughout the entire period, the beacon transmitted without interruption every hour with three exceptions--a 13-hour gap on January 21, a three-hour gap on April 27, and a 48.5-hour gap from May 29 to June 1. However, many of these transmissions turned out to be false readings, as they often registered the same position for days on end and therefore zero speed. These readings were removed from the analysis, leading to a slightly higher-than-expected value for the mean drift speed. The total distance traveled in the November-June period is 975.9 km, and the net displacement of the target is 599.3 km. In June, 7E drifts toward the west-northwest as it follows the southern Beaufort Sea coastline. The mean speed for the entire time interval is 6.0 km/day, and the median speed is 4.3 km/day. Drift speeds are somewhat variable throughout the

November-June time period, with a standard deviation of 6.3 km/day. The drift statistics of 7E are summarized in Table 4-1.

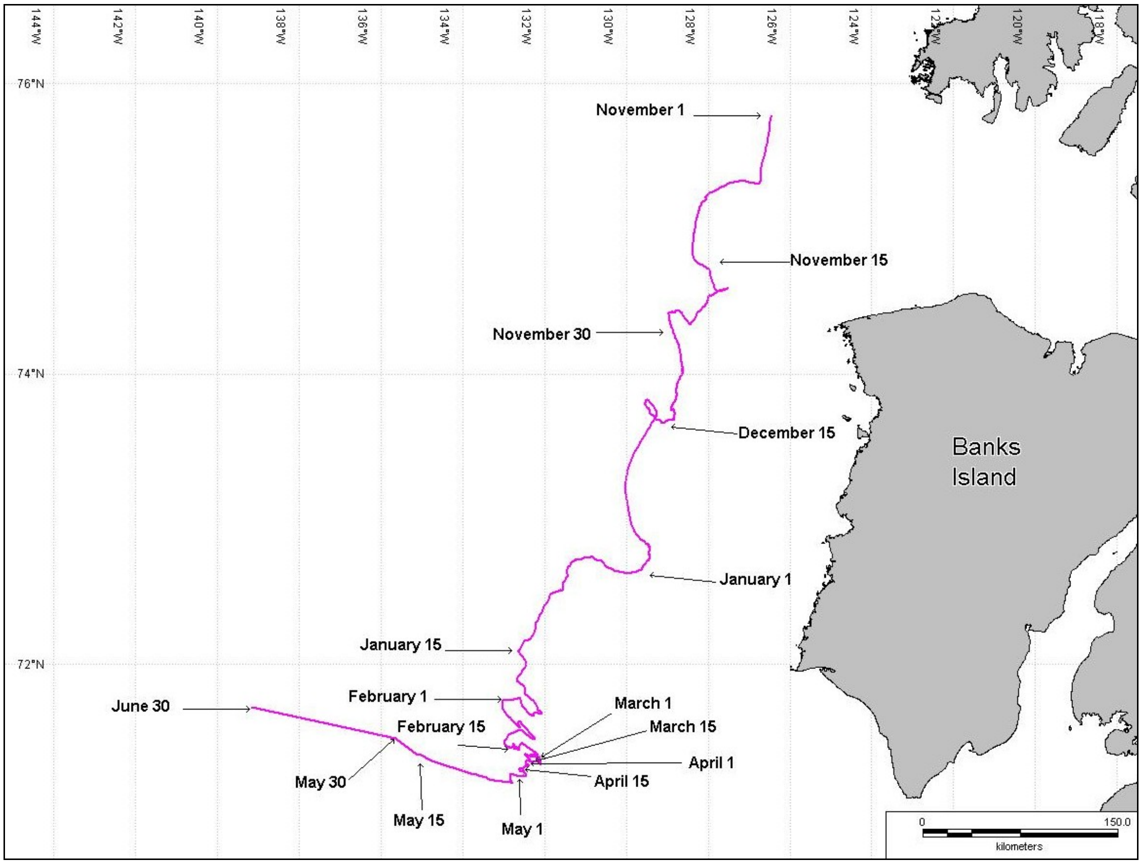

Figure 4-2: Drift track of beacon 7E for the period November 1, 2010 to June 30, 2011.

4.1.2 Target 1B

Figure 4-3 shows that from November 1 to November 17, 2010 Target 1B continued its overall southwest drift, moving from approximately 77° N to 76.1° N over the 17 days. Exceptions to the southwest drift account for only 27% of the period, and the target is never stationary. The total distance traveled by the target in the early-mid November period is 119.1 km, with a net distance covered of 112.2 km. The mean drift speed is 7.8 km/day, and the median speed is 5.8 km/day. Drift speeds vary somewhat, registering a standard deviation of 5.3 km/day. The drift statistics of 1B are summarized in Table 4-1.

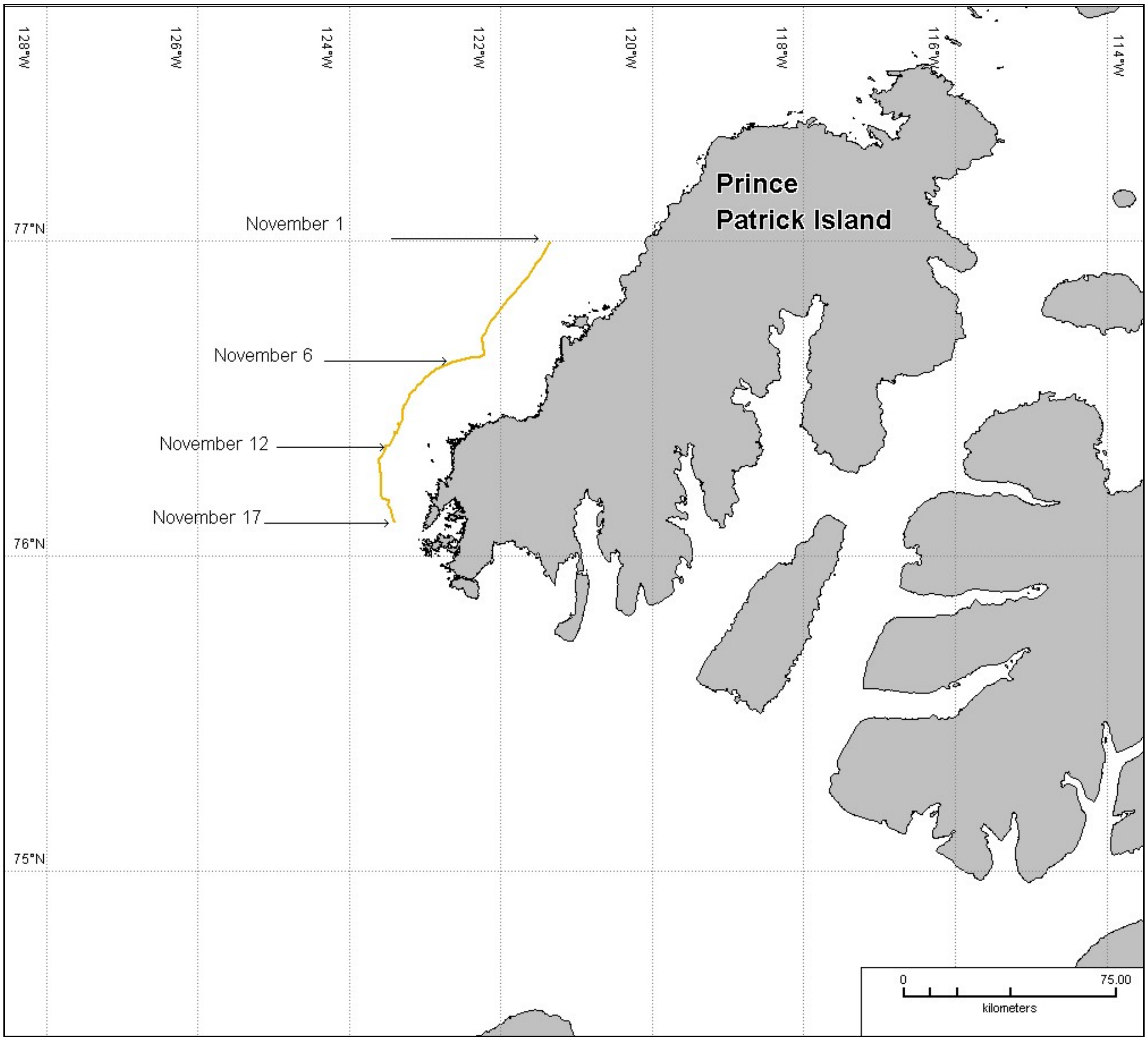

Figure 4-3: Drift track of Beacon 2E for the period November 1 – 17, 2010.

4.2 Drift Speed Analysis

The drift speed analysis was done following the guidelines of the previous project progress report. A set of three graphs are presented for each beacon:

1) Drift speed distribution. This graph is a vectorial representation of the ice drift speeds and directions. The distribution of this graph gives the preferential direction and the perturbations of the trajectories.

2) Frequency of the drift speed distribution. This graph gives the cumulative occurrences of each ice drift direction. This can help to clarify the preferred ice drift direction when the distribution tends to be uniform.

3) Exceedance probability of the drift speed. This graph presents the probability that an ice drift speed value can be exceeded. For instance, the 0 km/day speed value can be exceeded 100% of the time or there is 100% probability that any magnitude of the ice drift vector will be greater than 0 km/day. When the distribution of the data is so asymmetric that the mean value and the median are not close values, then the median is a better estimator since the mean value can be affected by even one value which is appreciably greater than the mean

4.2.1 Target 7E

Figure 4-4 shows the magnitude and distribution per direction of Target 7E instantaneous speed in km/day. Although the target's overall drift was to the southwest over the November-June time period, it sporadically drifted in many other directions, very briefly reaching its highest speeds toward the northwest. Figure 4-5 shows that the target's most frequent drift direction was toward the south and west.

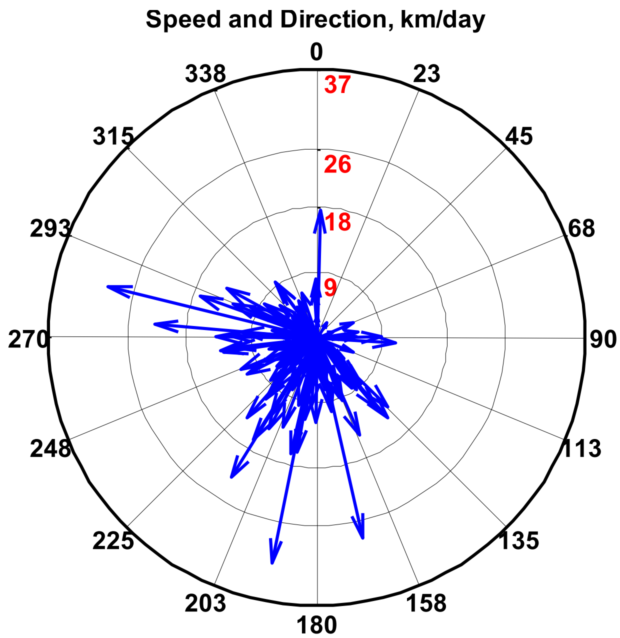

Figure 4-4: Drift speeds of Target 7E (red number) for the period November 1 2010–June 30, 2011.

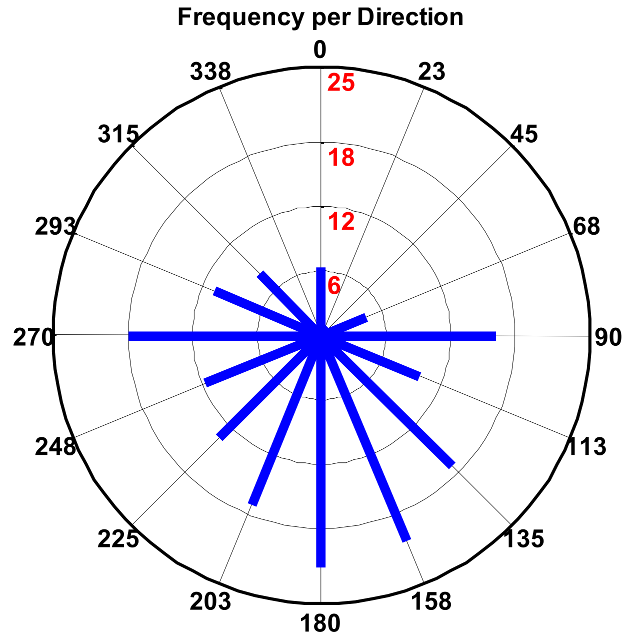

Figure 4-5: Frequency of the drift speed per direction (red number) for Target 7E for the period November 1 2010–June 30, 2011.

Figure 4-6 shows the exceedence probability where relatively large speed of the target is observed.

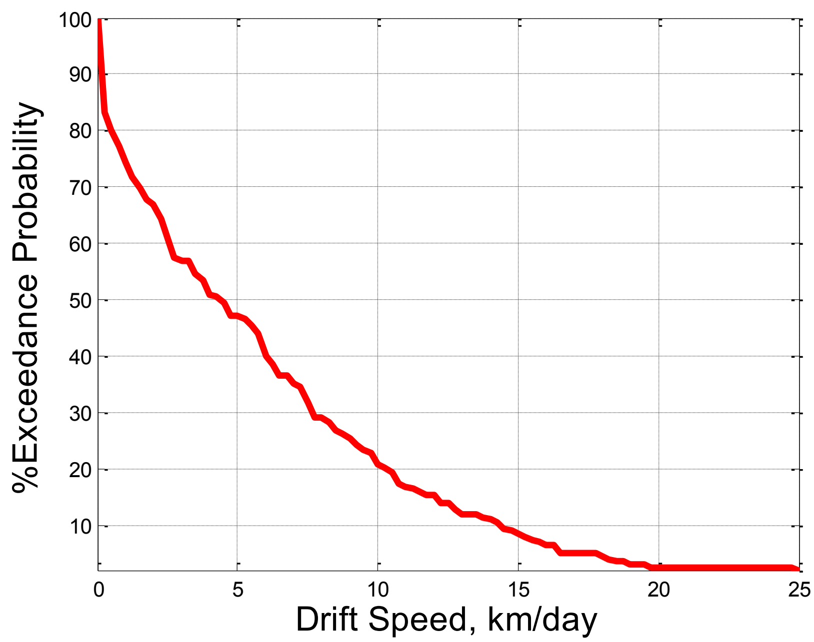

Figure 4-6: Exceedence probability of the drift speeds for Target 7E for the period November 1 2010–May 29, 2011.

4.2.2 Target 1B

Figure 4-7 shows the magnitude and distribution per direction of Target 1B instantaneous speed in km/day. The target drifts fastest and most frequently toward the southwest, and also drifts frequently toward the south (see Figure 4-8) at slower speeds.

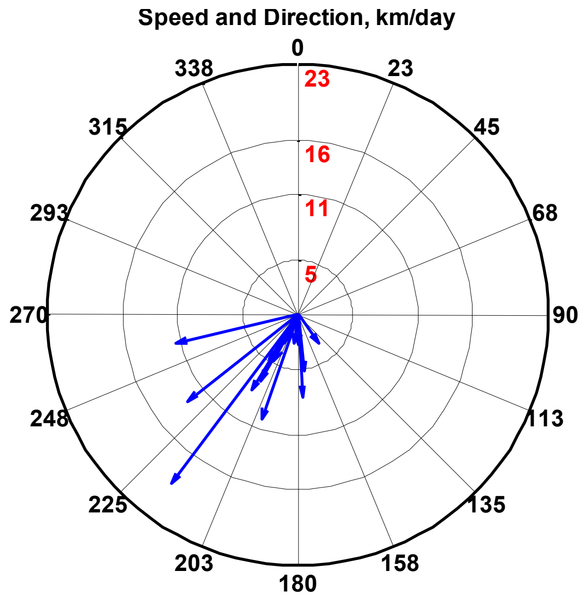

Figure 4-7: Drift speeds and associated azimuthal directions of Target 1B (red number) for the period November 1–17, 2010.

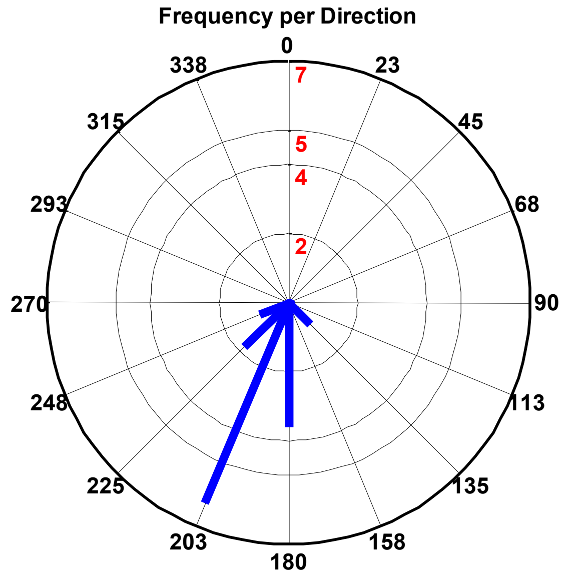

Figure 4-8: Frequency of the drift speed per direction for Target 1B (red number) for the period November 1–17, 2010.

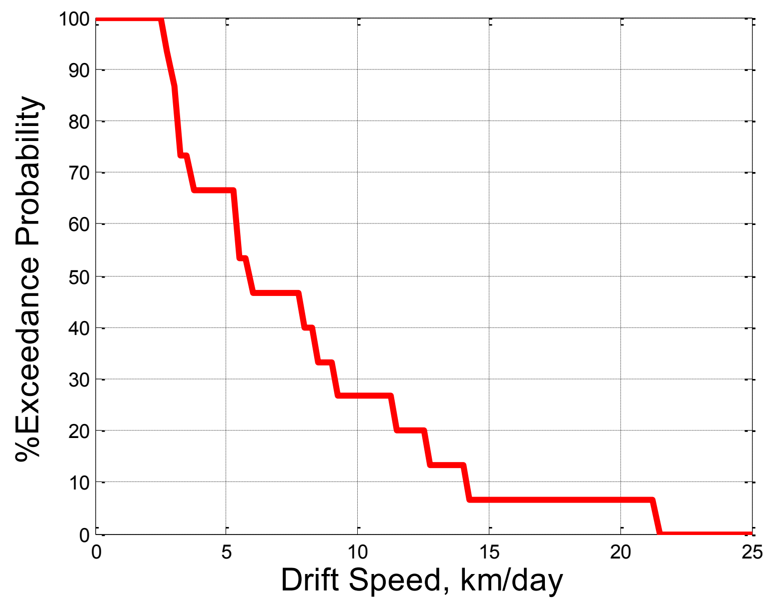

Figure 4-9: Exceedence probability of the drift speed for Target 1B for the period November 1–17, 2010.

4.3 Review

Target 1B drifts mainly southwest, and Target 7E drifts mainly toward the south-southwest, along the western margin of the Arctic Archipelago during the November-June time period (refer to Table 4-1 for drift statistics).

Table 4-1: Drift statistics for Targets 7E and 1B, November 1, 2010 to June 30, 2011.

Target	Mean Speed (km/day)	Median Speed (km/day)	Drift Speed St.Dev (km/day)	Total Distance (km)	Net Distance (km)	% of Time Period Spent Drifting in Non-SW Direction
7E	6.0	4.3	6.3	975.9	599.3	68%
1B	7.8	5.8	5.3	119.1	112.2	27%

Although Target 7E is further offshore than 1B and in deeper (greater than 200 m depth) water where it is more influenced by the Beaufort Gyre and less influenced by the coastal boundary effects, its mean and median drift speeds during this period are somewhat slower. However, this is skewed by the fact that 7E's transmission record covers the entire November-June period, whereas 1B's much shorter record extends only through mid-November. Target 7E eventually turns toward the west-northwest as it reaches the southern Beaufort Sea, and continues roughly paralleling the shoreline. The drift of both targets is consistent with the circular flow of the Beaufort Gyre toward the southwest along the Archipelago's western margin, then to the west in the Southern Beaufort Sea. The abrupt west-northwest turn in the drift of Target 7E is noteworthy, and further study of ice motion in the vicinity of the lease areas is warranted. While we have so far observed one ice island to turn to the west before reaching the lease areas further to the south, if we were to observe this drift pattern repeatedly in the Southern Beaufort Sea, we may be able to draw conclusions about the likelihood of such ice floes affecting (or not affecting as the case apparently may be) operations in the lease areas. As of now, the drift of Target 7E alone is not a statistically significant sample.

5 IMAGE ANALYSIS

5.1 Visual Analysis of Features

As indicated in Section 3.2, the original intent was to acquire images on a monthly basis, for Target 7E, which was the only one left during the current period. This was achieved for both April and May 2011. No images were collected in June due to scheduling conflicts experienced by CIS, and because of the intermittent transmissions of the beacon on Target 7E which made it impossible to locate the image when required.

5.1.1 Target 7E

Two images were obtained of this target.

April 2011 Imagery

A Fine Quad RadarSat-2 image taken on April 11, 2011 contained Ice Island 7E which broke out in early August 2008. This Ice Island has been tracked and monitored since July 2009. This feature has a distinct surface signature in terms of texture and tone across its extent, with its northern part (in Figure 5-1) dominated by marine re-entrant ice, while its southern portion is composed of shelf ice.

Figure 5-1 shows fracturing of the Target 7E at the time of the image with 1 major fragment detaching from its left hand side (fragment #8). The fragments surrounding the target originate largely from the marine ice portion of the original Ice Island as these fragments have the same tone, texture, and period length as the parent Ice Island. This is an interesting finding which suggests that the weaker portion of Ice Island, in terms of structural strength, is the marine ice portion.

The 7E target, shown in Figure 5-1, has a distinct rib texture (180 m period) and rough surface. In the figure below, all shelf targets are outlined in yellow, and Table 5-1 below the image lists the size (area – km^2), origins, current conditions, and notable characteristics of the Ice Island and its surrounding fragments on April 11, 2011.

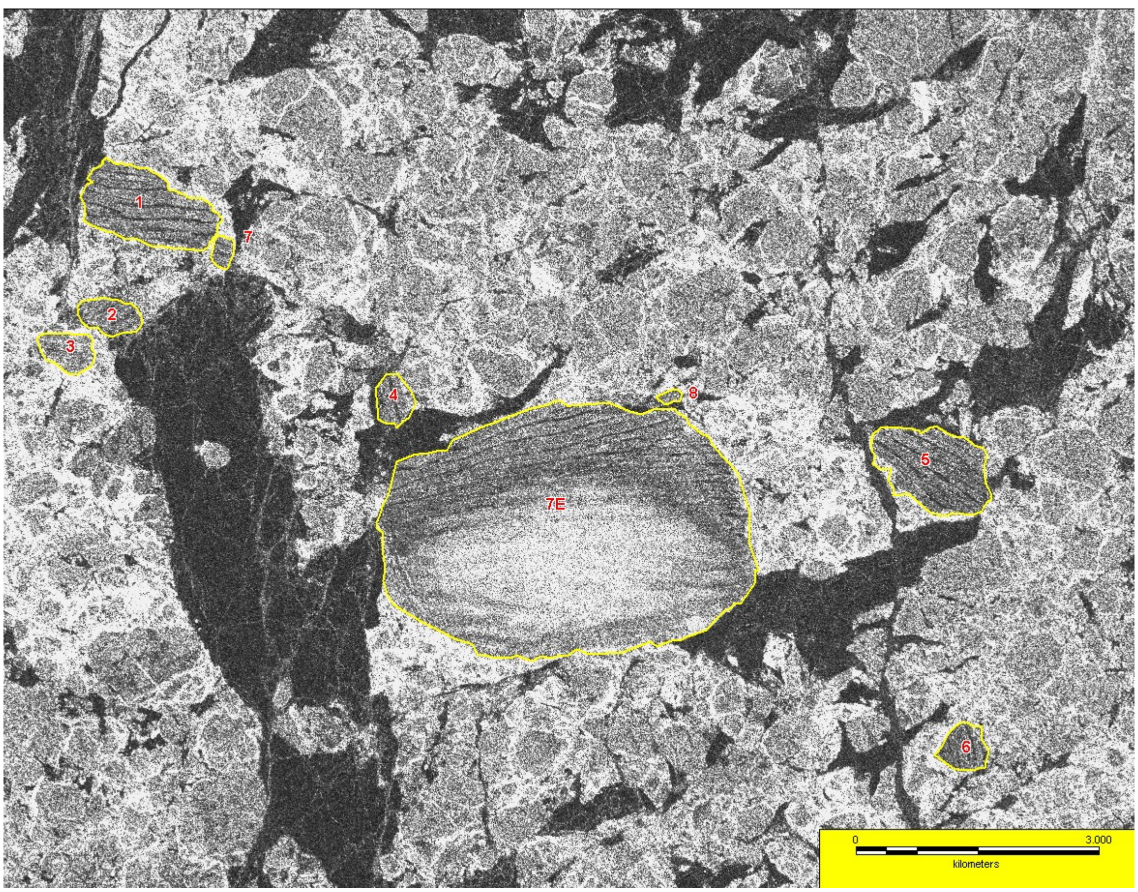

Figure 5-1: April 11, 2011 RadarSat-2 FineQuad (HV) of Target 7E.

Table 5-1: 7E and fragment Size, Features, Conditions, and Features on April 11, 2011.

Target	Size (km^2)	Origin	Condition	Features
7E	11.74	Markham	Fragments around; drifting away to W	Marine and classic shelf portions
1(Son of 7)	1.28	Markham	Actively fracturing Fragments to W	Marine Ice type
2	0.27	Son of 7	Recently fractured (weak) Drifting SSW away from parent	Medium period (180m)
3	0.26	Son of 7	Ragged, weak; drifting S of parent	Marine Ice type
4	0.23	7e	recently fractured NW of parent	Angular, weak
5	1.17	7E	No fractures NE of parent	Rounded form (strong?)
6	0.27	7E	No fractures Drifting away to E	Rounded form
7	0.08	Unkn	Detached rib Drifting away to SSW (classic, not marine type)	No fractures 230m period
8	0.03	Unkn	Detached rib Off to SE. (classic, not marine type)	No fractures 270m period

Figure 5-2 shows an area distribution histogram of the main target and its fragments.

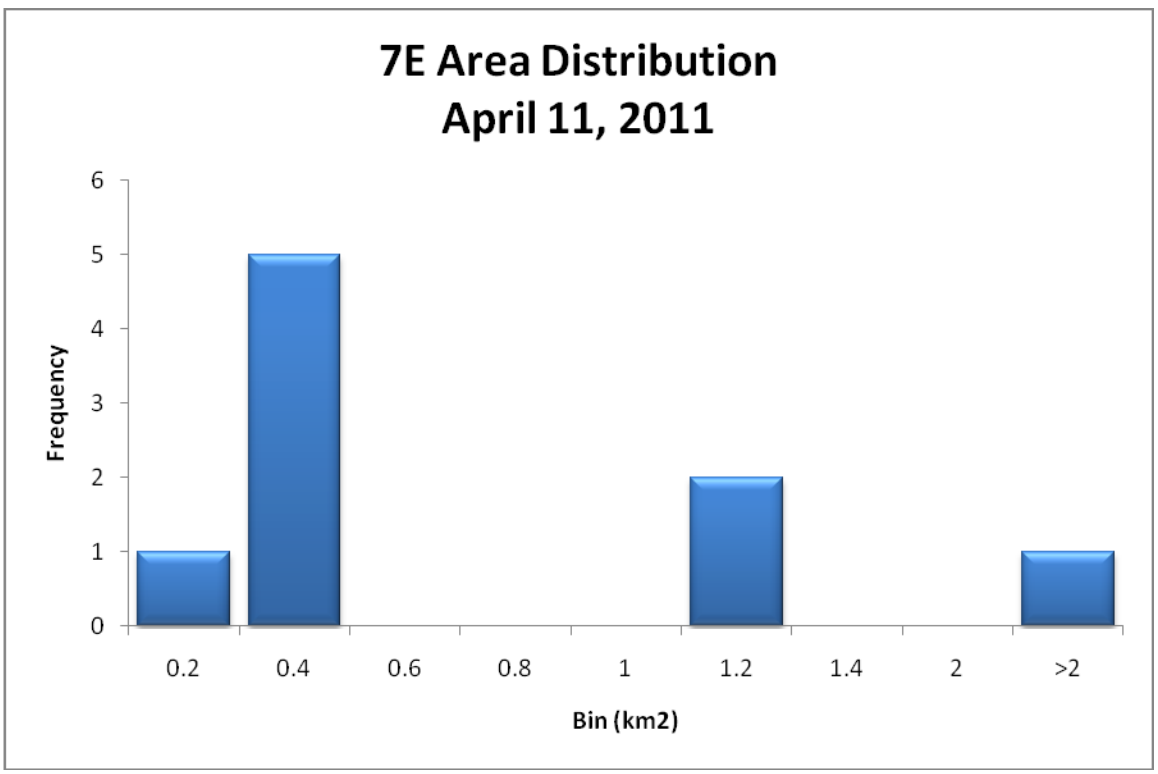

Figure 5-2: Area Distribution Histogram plot of Ice Island 7E and its surrounding fragments on April 11, 2011.

The area distribution histogram for Target 7E and its surrounding fragments shows the Ice Island 7E of 11.63 km^2 in the >2km^2 bin. The majority of Ice Island fragments are small with areas of 0.4 km^2 and less, with one having an area of 1.3 km^2.

We show the fracturing pattern of these fragments occurs along defined longitudinal ribs of the main Ice Island. It can be speculated that the splintering of the fragment in this way occurs along the trough of the rib. The mechanisms of this process are currently unknown; however, ice weakness in the trough portions of an undulation would facilitate a higher probability of ice fragmentation and break-up in this part of the Ice Island. We further show multiple fractures in Features 7 and 8 with, what appears to be, active break-up occurring at the time of the image. The fractures in these features have not formed longitudinally, rather detached in more of a block type pattern from the parent Ice Island. It is anticipated that future break up will generate numerous small angular fragments from Features 1 and 5.

May 2011 Imagery

This RadarSat-2 Fine Quad image from May 15 contains the Ice Island Target 7E, and the smaller Ice Island referred to as Son of 7 (see Figure 5-3). In addition, 6 Ice Island fragments and 1 small Ice Island recently fractured off 7E are also evident.

Figure 5-3 shows significant fracturing of the Target 7E with 4 major fragments detaching from the bottom right portions of the target. Shown below is the radar image with all shelf targets outlined in yellow. Table 5-2 below the image lists the size (area – km^2), origins, current conditions, and notable characteristics of the Ice Island and its surrounding fragments on May 15, 2010.

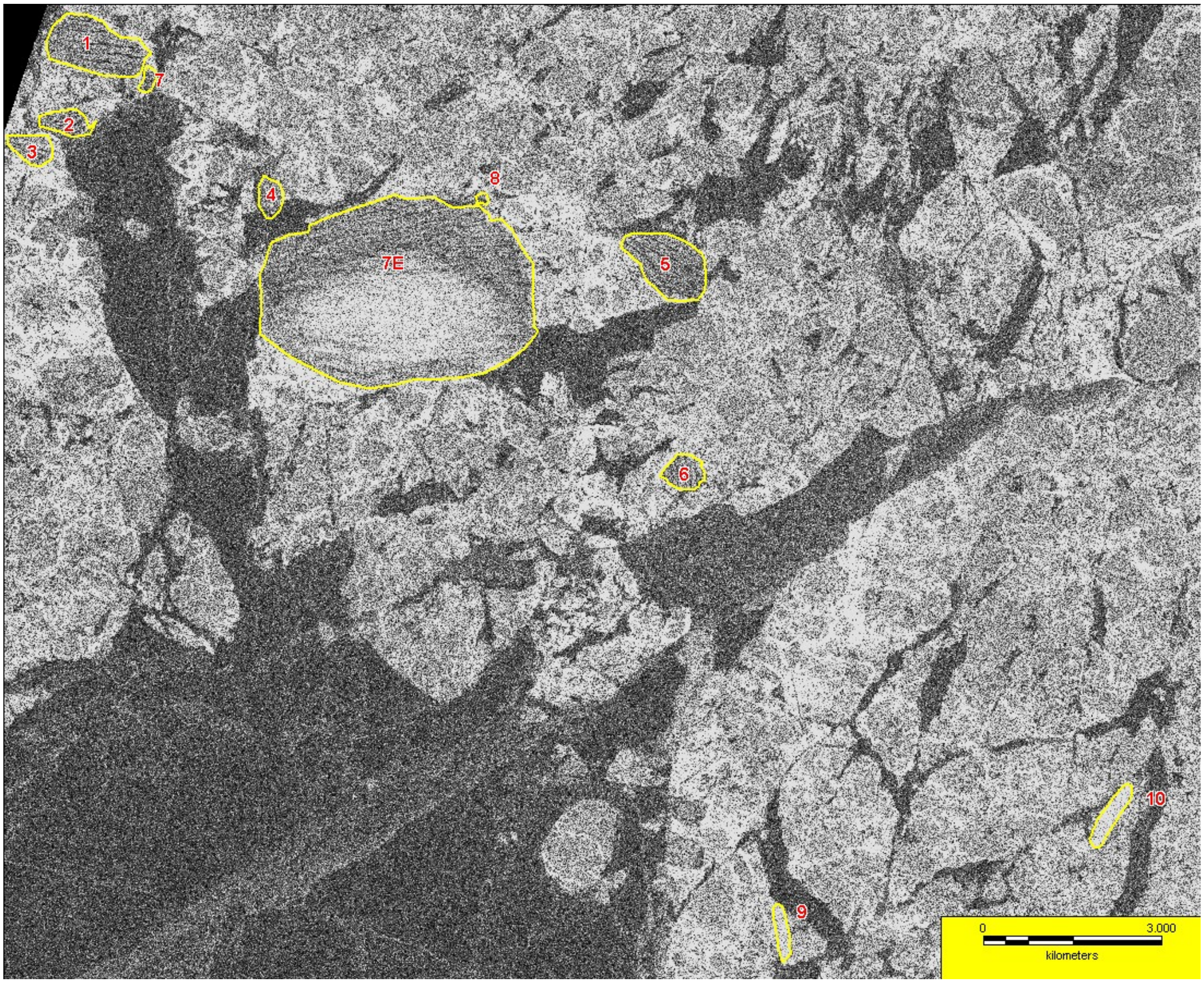

Figure 5-3: May 15, 2011 RadarSat-2 FineQuad (VH) of Target 7E.

Table 5-2: 7E and fragment Size characteristics, conditions, and characteristics on May 15, 2011.

Target	Size (km^2)	Origin	Condition	Features
7E	11.63	Markham	Fragments drifting W and E	Marine and classic shelf portions
1 (Son of 7)	1.20	Markham	Actively fracturing; Fragments to S	Marine type
2	0.27	Son of 7	Recently fractured (weak); Drifting SSW away from parent	Medium period (180m)
3	0.28	Son of 7	Ragged, weak S of parent	Marine type
4	0.22	7E	recently fractured NW of parent	Angular, weak
5	1.08	7E	No fractures NE of parent	Rounded form
6	0.31	7E	No fractures Drifting away to E	Rounded form
7	0.08	Unkn	Detached rib Drifting away to SSW (classic, not marine type)	No fractures 230m period
8	0.03	Unkn	Detached rib Off to SE. (classic, not marine type)	No fractures 270m period
9	0.17	Unkn	Detached rib Drifting away to SSW (classic, not marine type)	No fractures; 230m period
10	0.27	Unkn	Detached rib Off to SE (classic, not marine type)	No fractures; 270m period

An area distribution histogram is provided below (see Figure 5-4) of the main target and its fragments.

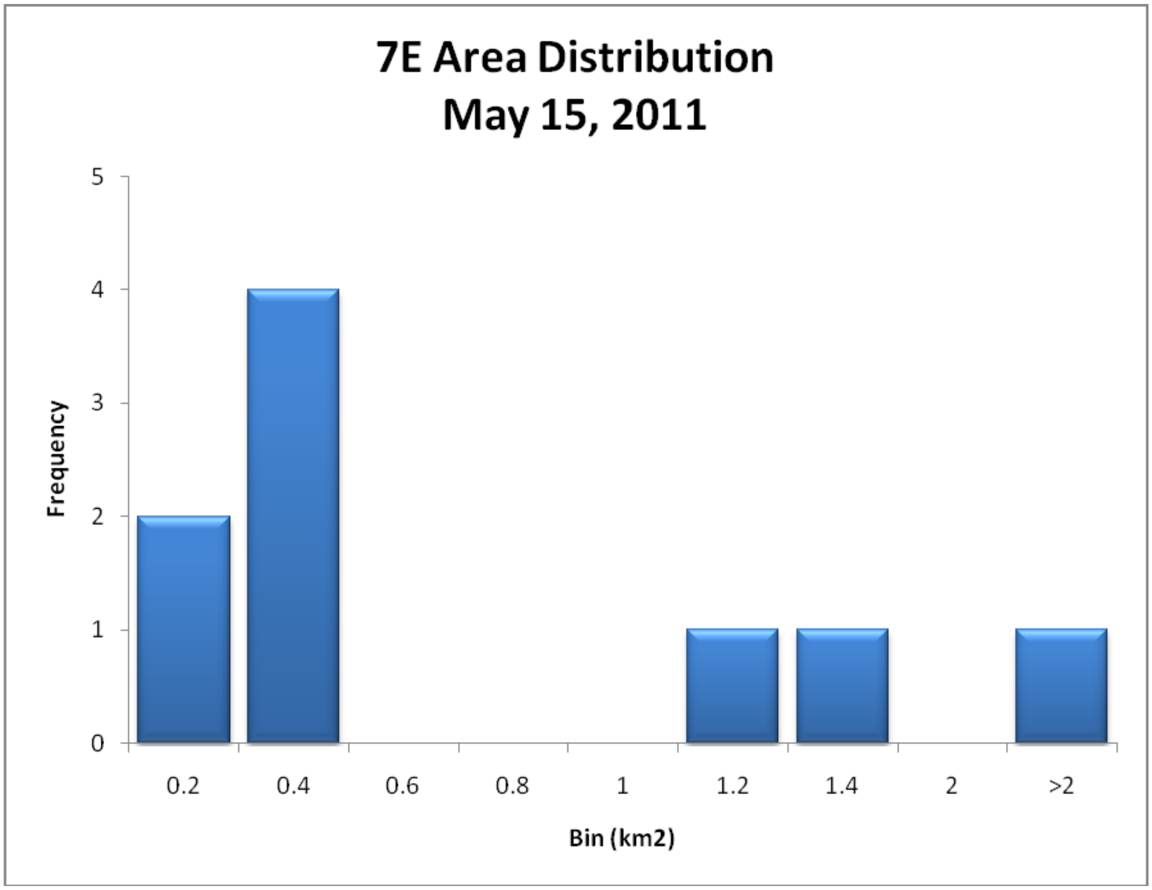

Figure 5-4: Area Distribution Histogram plot of Ice Island 7E and its surrounding fragments on May 15, 2011.

Figure 5-4, the area distribution histogram for Target 7E and its surrounding fragments shows the Ice Island 7E of 11.41 km^2 in the >2km^2 bin. The majority of Ice Island fragments are small with areas of 0.5 km^2 and less, with 2 having areas of 1.08 and 1.20 km^2 respectively. As with the previous analysis on April 11, 2011, this frequency plot suggests that the Ice Island fragments rapidly break down to a relatively small size at the time of calving from the main Ice Island. Similarly with the June example, in the case with July, Fragments 7 and 8 suggest that elongated sections of Ice Island (a rib) breaks free from a plane of weakness via the main Ice Island.

5.2 Review

In the second report, we suggested there might be a set of relatively stable sizes for Ice Islands as they drift, around the 5 km^2 size, and as they break up, the resulting fragments might have stable sizes. The Ice Islands we are monitoring appear to be about 0.2 to 11.6 km^2 in area. We do not have a statistically significant sample, but this might be a relatively "stable" size of Ice Island, in the current conditions. The data from the present report indicates that the Ice Island and reentrant ice fragments appear to break up rapidly to very small sizes, less than 0.4km^2 in area. Many of these fragments could be a threat to an offshore structure and are unmanageable Ice Features.

6 PROCESSES OF ACCRETION AND DECAY

This chapter describes changes in size and shape using the data available from Target 7E. Target 1B was not analyzed, because, as indicated earlier, the beacon only lasted for a little more than 2 weeks and consequently no images were obtained.

6.1 Changes in Size

Table 6-1 summarizes area changes for Target 7E. The changes in area represent the fall, winter and spring period from September through May 2011. Total area change calculations are based on the changes for the Target 7E.

Table 6-1: Time Series Summary of Area Changes for Target 7E.

Image Acquisition Date (DD-MM-YY)	Target	Area (km^2)	Area Change (km^2)	% Change from April 2010
12-Sep-10	7E	11.85		
11-Apr-11	7E	11.74	-0.11	-0.93
15-May-11	7E	11.63	-0.11	-0.94
		Change from April – May	**-0.22**	**-1.86**

The data in Figure 6-1 are presented in the graph below to show how changes in area occur over time. From this graph we can see that Target 7E has decreased by about 0.25 km^2 over the current analysis period.

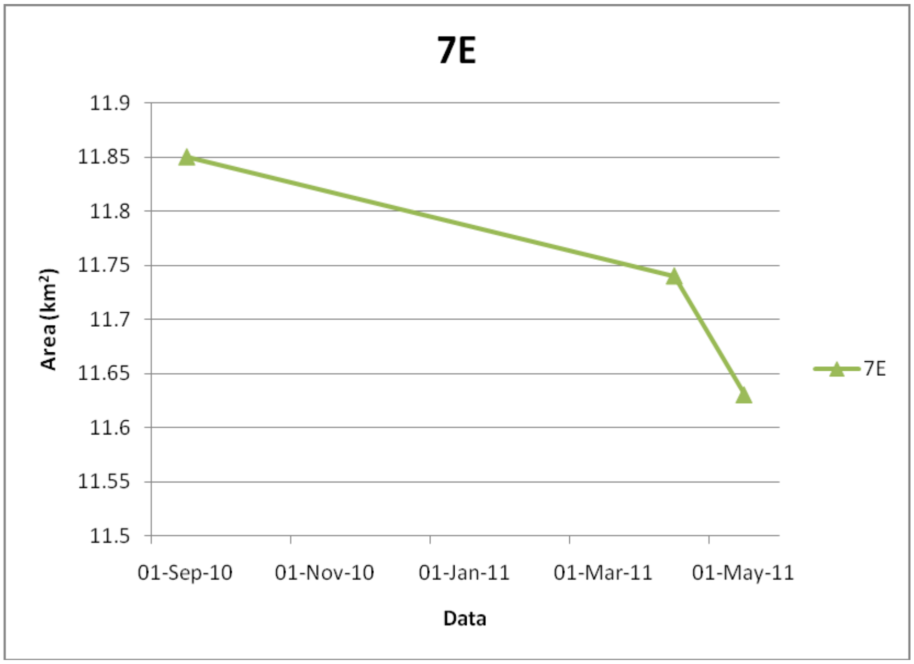

Figure 6-1: Area changes from September 2010 through May 2011.

These changes in size are more evident when the graph plots percentage change from the original size, see Figure 6-2.

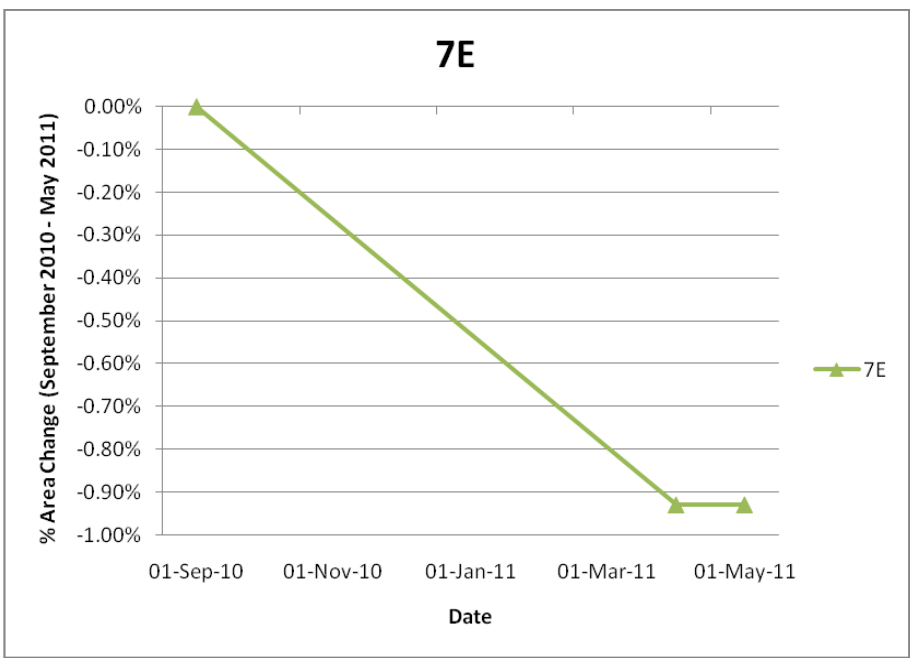

Figure 6-2: Percent Area Changes from September 2010 through May 2011.

6.2 Area Changes by Location

Analysis shows that the pattern and frequency of disintegration decreased throughout the winter freeze up and spring thaw period when compared with the summer melt period before as the winter pack ice concentration increased. Over the summer the rate of disintegration is about 0.76 km^2/month (June – September, 2010) whereas over winter the rate is 0.02 km^2/month (September 2010 – May, 2011). This pattern follows expectations. For the period of November 1, 2010 to May 15, 2011, Target 7E drifted from the M'Clure Strait Zone towards the Banks Island zone, eventually arriving in the Beaufort Sea. Since imagery of the target was only acquired in April and May in the Beaufort Zone only, we are unable to produce a map as we have in previous reports showing Area changes as a function of location.

6.3 Shift in Area Balance by Feature

The analysis immediately above refers only to the area changes of the main Target 7E. As described in the previous report, during drift into the Beaufort, the nature of the hazard changes from a single feature to a smaller feature surrounded by a swarm of fragments. Therefore, we need to measure the progressive changes in area between these - the main feature and its fragments. As indicated in the previous report, we have a lower cutoff size for fragments, 200 m (referring in the case of Ice Islands, to the long dimension). In this report, we extend the histograms to include two new columns, one for fragments smaller than 200m and the last one, to measure all the remaining unaccounted area which is either too small to measure, has completely disintegrated or has moved out of the frame of the image. The resolution of the imagery is 8 m, so we can identify floes as small as 200 m. However, when ice pieces from the ice island get this small, they no longer have any characteristic features (such as the surface rills) that allows one to identify them as fragments of an ice island.

Based on the most recent June-September set of imagery of Target 7E, we show Figure 6-3 and Figure 6-4. The "Unaccounted" column is based on the area of Target 7E on September 1m 2010, minus the area now and the area of all fragments over 200m.

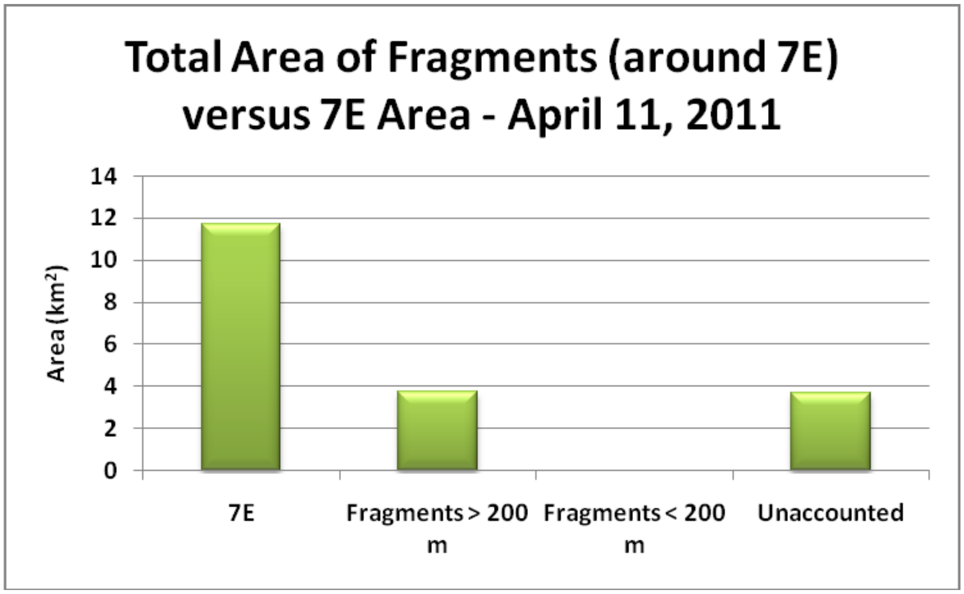

Figure 6-3: Bar graph of Total Area of Ice Island 7E and Total Area of surrounding fragments on April 11, 2011.

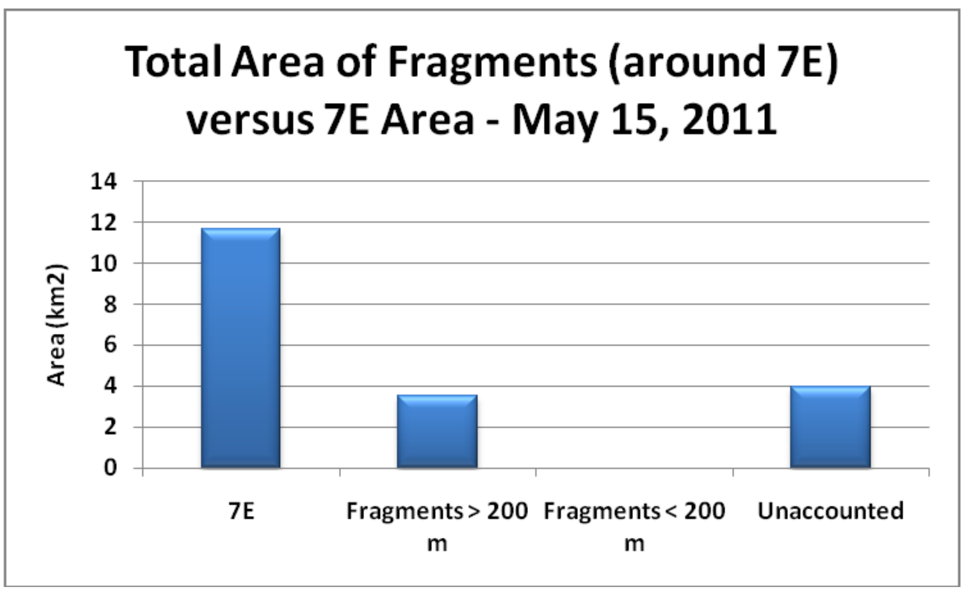

Figure 6-4: Bar graph of Total Area of Ice Island 7E and Total Area of surrounding fragments on May 15, 2011.

It is interesting to note that in no case did we see fragments smaller than the 200m in this series of images. The numbers between April and May are similar for all categories considered.

6.4 Changes in Shape

Figure 6-5 below provides an overlay image sequence of Target 7E starting on April 11 through May 15, 2011.

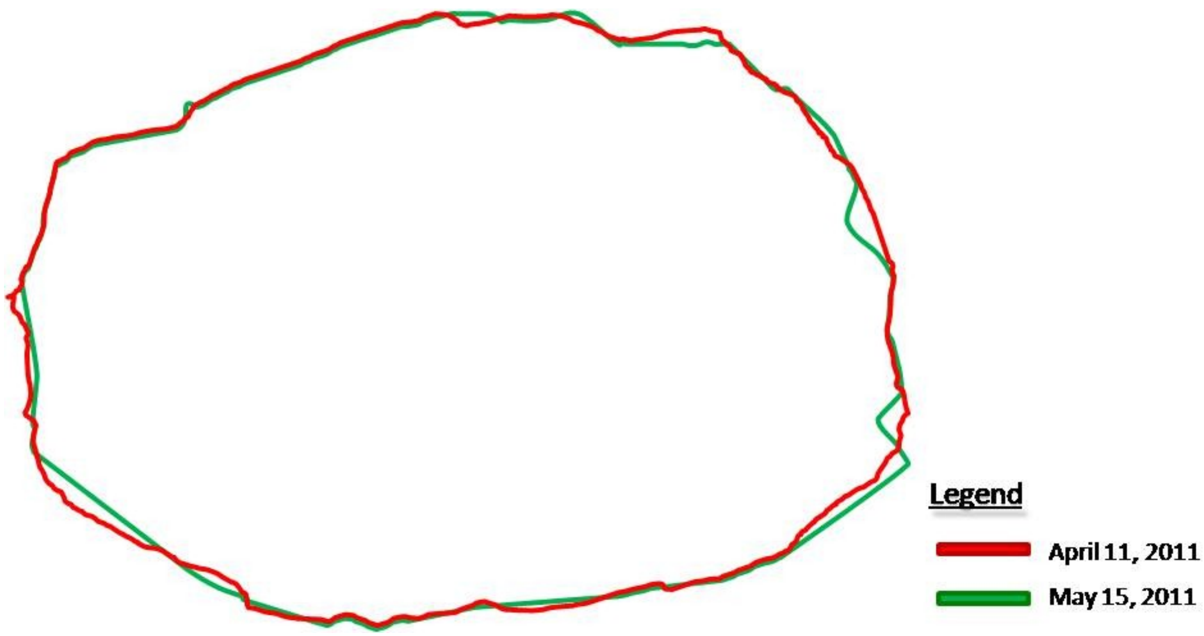

Figure 6-5 Overlay for Target 7E Imagery from April 11(red) through May 15 (green) 2011.

Target 7E has undergone very minor changes in terms of both area change, and shape alteration over the course of our 1 month analysis period shown in the outlines in Figure 6-5. From April (Red outline) to May, 2011 (Green outline), 7E appeared to be fracturing and losing mass on its extremities, chiefly along the right hand and top portions of the target. The shape is generally becoming more rounded. In terms of drawing more conclusions regarding shape changes, given the imagery and our techniques, this sort of analysis is at the limits of its scope in terms of accuracy and resolution.

6.5 Summary

Target 7E has continued to decrease in size and has lost some of its characteristic angular features. FineQuad imagery is good enough to depict general trends, when good imaging circumstances occur, but UltraFine is necessary to advance our understanding further.

7 Clustering & Dispersion

As a continuation of the clustering and dispersion analysis of ice fragments around Ice Island 7E presented in the third report, two Radarsat-2 images taken on April 11 (Figure 7-1) and May 15, 2011 (Figure 7-2) have been analyzed. Each image displays ice island 7E surrounded by numbered ice fragments, also outlined in yellow. Only one "cluster" has been visually identified in both images, and this cluster is defined by a red-outlined oval drawn through the fragments within the cluster in both images. The cluster is composed of the same fragments in both images. In the May 15 image, two new fragments (numbered 9 and 10) appear that are not seen in the April 11 image due to the size of that image--these two fragments were excluded from the analysis so that only fragments visible in both images are used.

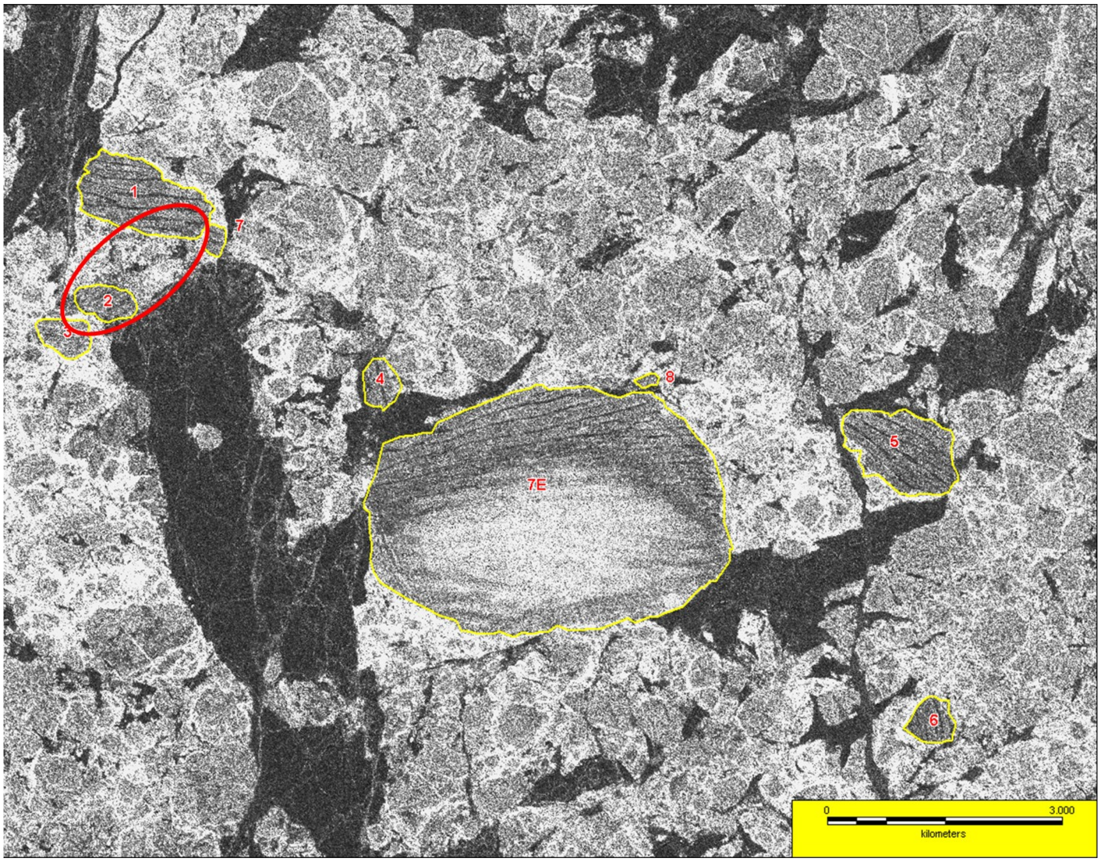

Figure 7-1: Radarsat-2 image taken on April 11, 2011 showing ice island 7E and surrounding fragments.

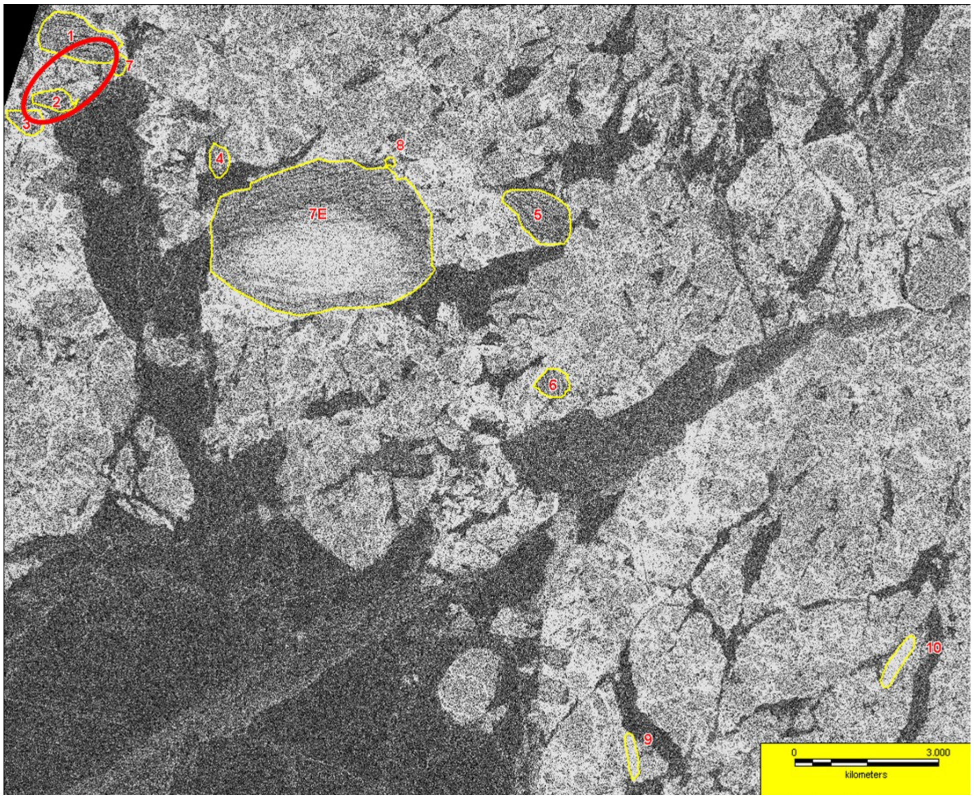

Figure 7-2: Radarsat-2 image taken on May 15, 2011 showing ice island 7E and surrounding fragments.

Table 7-1 below shows the lengths of the major and minor axes of the ellipses, which have been hand-drawn through the fragments of the cluster in each image. All distances in this analysis are based on a projection of the two images into a northern polar stereographic projection.

Table 7-1: Lengths of the major and minor axes of ellipses drawn through the cluster in each image.

Date	Major Axis (m)	Minor Axis (m)
April 11, 2011	2057	1161
May 15, 2011	2045	1203

As in the third report, we compute the parameter S_i, which is a quantitative measure of the degree of scatter within the cluster, from the Davies-Bouldin index (DBI). The parameter is essentially the standard deviation in the distances from each member of a cluster to the cluster centroid. A second parameter from the DBI, M_{ij}, is a measure of separation between two clusters; however in this analysis, we have used it to indicate the separation between the cluster and the ice island, and between individual fragments and the ice island, for those fragments not lying within an identifiable cluster. Between the ice island and a single floe, the parameter M_{ij} simply becomes the separation distance. Finally, the location of the cluster or a single fragment relative to the ice island can be represented by the azimuthal bearing from the ice island to the cluster or fragment centroid. Table 7-2**Error! Reference**

source not found. shows the two DBI parameters and bearing of the cluster and each fragment in each image, and the means and standard deviations (StD) of these parameters for the cluster and other outlying fragments in a given image.

Table 7-2: Various parameters for ice island fragment cluster and fragments (see text for details of parameters quoted).

Date	Cluster/ Fragment	Si (m)	Mij (m)	Bearing from 7E (°)	Mean Si (m)	Mean Mij (m)	Mean Bearing (°)	Si StD (m)	Mij StD (m)	Bearing StD (°)
April 11, 2011	1-3, 7	1027	12389	316	1027	5563	43	0	4120	53
	4	Single floe	2578	320						
	5	Single floe	4828	94						
	6	Single floe	5886	133						
	8	Single floe	2136	54						
May 15, 2011	1-3, 7	1024	12755	317	1024	5564	45	0	4273	52
	4	Single floe	2660	323						
	5	Single floe	4602	96						
	6	Single floe	5695	136						
	8	Single floe	2106	57						

Conclusions that can be drawn from the data presented in Table 7-2 are the following:

- The cluster became more compact between April and May. It appeared to move slightly slower than the ice island, as its azimuthal angle relative to 7E increased by 1°.
- The cluster moved further away from the ice island between April and May, and the other fragments overall became further away from 7E, with their distances from the ice island becoming more variable with time.
- The bearing from the ice island to the fragments grew more uniform with time.

7.1 Relative Motion of Fragments

Figure 7-3 shows the motion of fragments in the cluster from April 11 (red dots) to May 15 (blue dots), relative to the ice island 7E, and Figure 7-4 shows the motion of fragments within the cluster, relative to fragment 1, the largest fragment in the cluster.

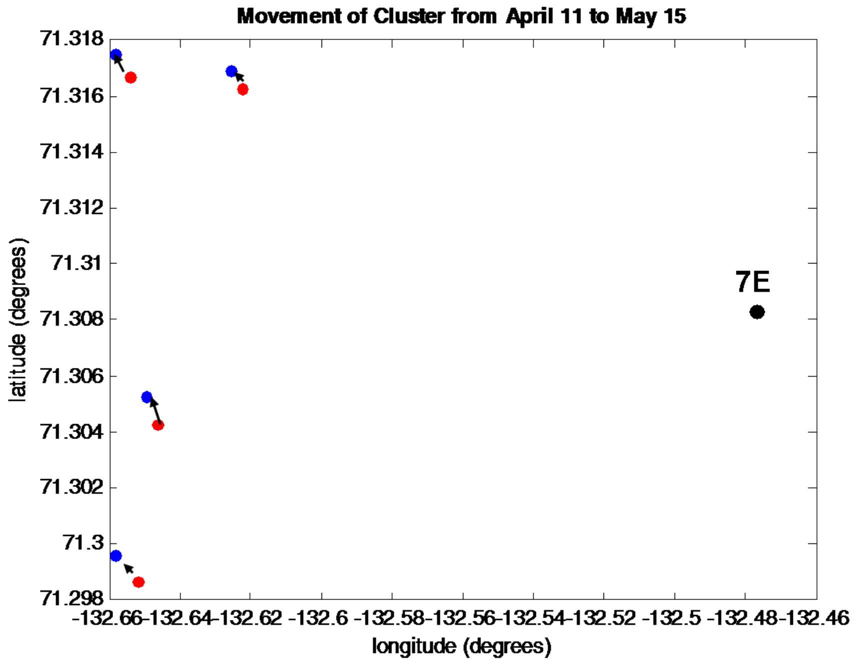

Figure 7-3: Comparison of drift of the cluster from April 11 (red marks) to May 15 (blue marks) relative to Ice Island 7E.

Figure 7-3 indicates that the cluster drifted slightly slower than the ice island from April to May. Figure 7-4 shows that two of the smaller fragments (fragments 2 and 3) within the cluster drifted closer to the largest fragment overall, with fragment 2 drifting to the northeast relative to fragment 1, and fragment 3 drifting to the west relative to the largest fragment. Fragment 7 drifted further away, to the east-southeast relative to fragment 1.

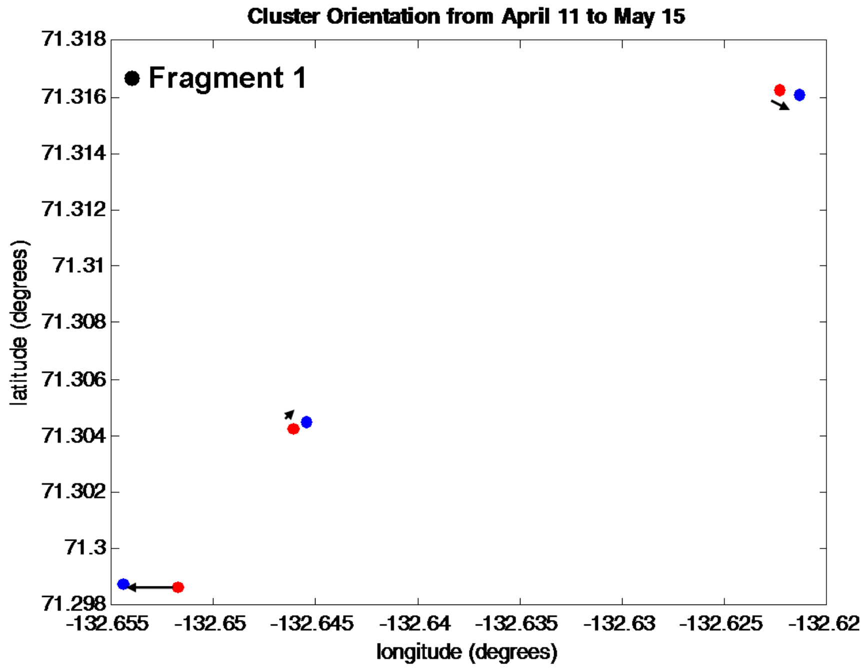

Figure 7-4: Relative motion of fragments 2, 3, and 7 within the cluster to the largest fragment 1 from April 11 to May 15.

7.2 Summary and Conclusions

- The cluster of smaller fragments moved slower than the larger ice island. Within the cluster, the smaller fragments moved closer to the largest fragment, and therefore moved slower than it and made the cluster more compact with time. The first conclusion is consistent with the last report, in which the clusters were also found to move slower than the larger parent ice island. However, the second conclusion is in contrast to the last report, in which it was found that the smaller fragments within the clusters appeared to drift faster than the largest fragment and made the cluster more disperse with time.

- The fact that the cluster moved slightly slower than the parent ice island indicates that a cluster of smaller ice fragments could present a hazard to a vessel or offshore structure immediately after the main ice island does so.

- Given the different results in this study compared to those from the ice fragment clustering and dispersion analysis in the last report, we cannot draw conclusions at this time about how ice fragment clusters will behave in terms of shape, size, and distance and bearing changes to their parent ice island with time. Despite the fact that both reports showed the clusters moving slower than the ice island over time, we do not yet have a statistically significant enough sample to conclude that this will always happen. Further study of this subject may help to advance our understanding of how clustering and dispersion of the ice island fragments evolve with time and drift.

8 OVERALL PROJECT SUMMARY - DRIFT ANALYSIS

8.1 General Situation

Figure 8-1 shows the drift of all targets between May 19, 2009 and June 30, 2011. In the following sections, we describe the movement of each beacon separately and analyze the patterns and statistical properties of each trajectory over this time period. For the same reasons discussed in Chapter 4, only positions approximately every 24 hours are used in this analysis, with all speeds converted into km/day.

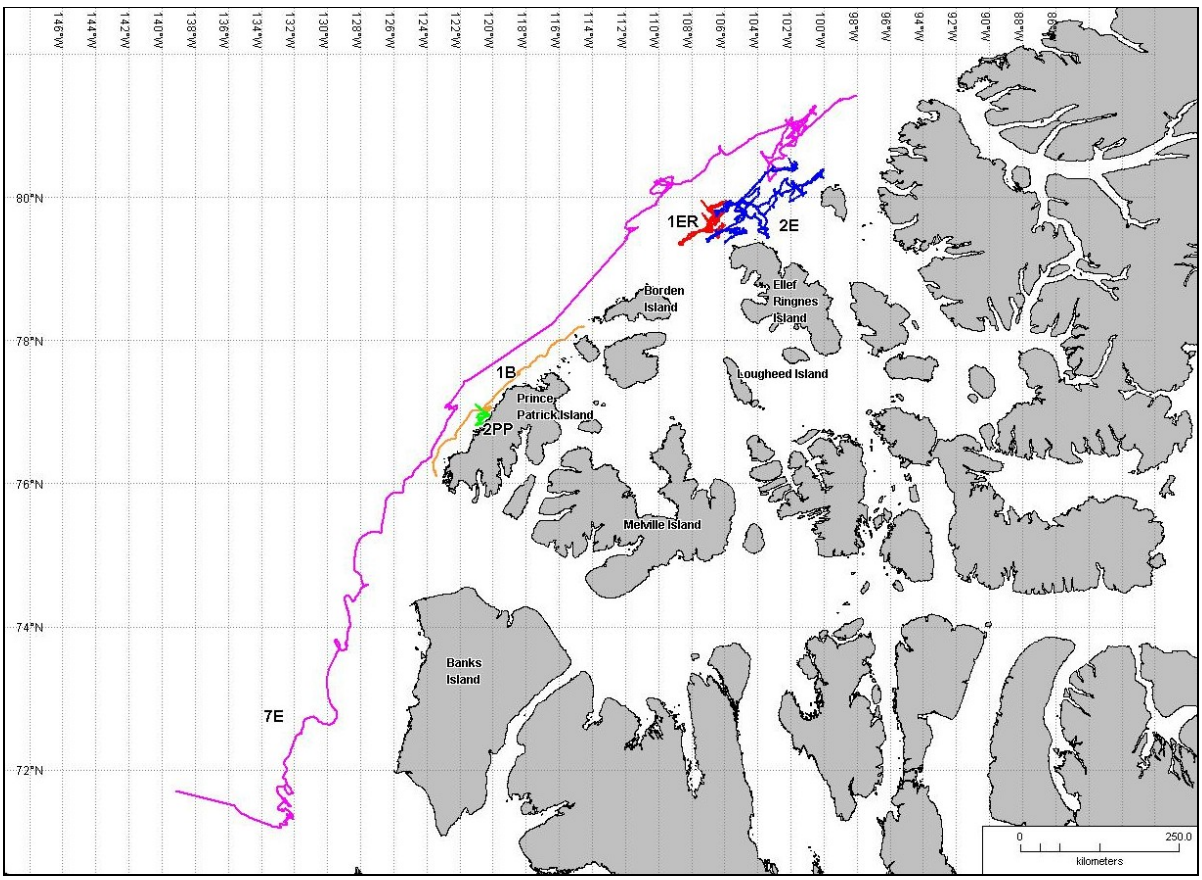

Figure 8-1: General Drift of all Targets from May 19, 2009 through June 30, 2011.

8.1.1 Target 7E

Figure 8-2 shows that during the time period July 11, 2009 to June 30, 2011, Target 7E (an Iridiumbeacon with 2.5 m accuracy) maintained a general south-southwesterly drift, moving from approximately 81.4° N to 71.7° N. Exceptions to the overall south-southwesterly drift (e.g., drift in a direction not between 180° and 225°) account for 73% of the entire beacon record, and are relatively evenly distributed in time. Drift not occurring between 180° and 270° (drift not toward the southwest) accounts for 57% of the beacon record. However, the target drifts to the south-southwest as its highest drift speeds are recorded in this direction. The total distance traveled between July 2009 and June 2011 is 2142.2 km, with a net drift distance of 1452.9 km. The mean drift speed for the entire July 2009-June 2011 time period is 4.5 km/day, and median speed is 2.7 km/day. Drift speeds throughout the entire beacon record time period are somewhat variable, with a standard deviation of 5.1 km/day. Drift speeds tend to range between 8 and 15 km/day during the summer months, and tend to be less than 8 km/day during the winter months, for about the first 250 days of the beacon record. Afterward, for the remainder of the beacon record, summer drift speeds tend to be slightly higher in the more southerly latitudes, ranging mainly between 10 and 18 km/day. Drift statistics for Target 7E are summarized in Table 8-1.

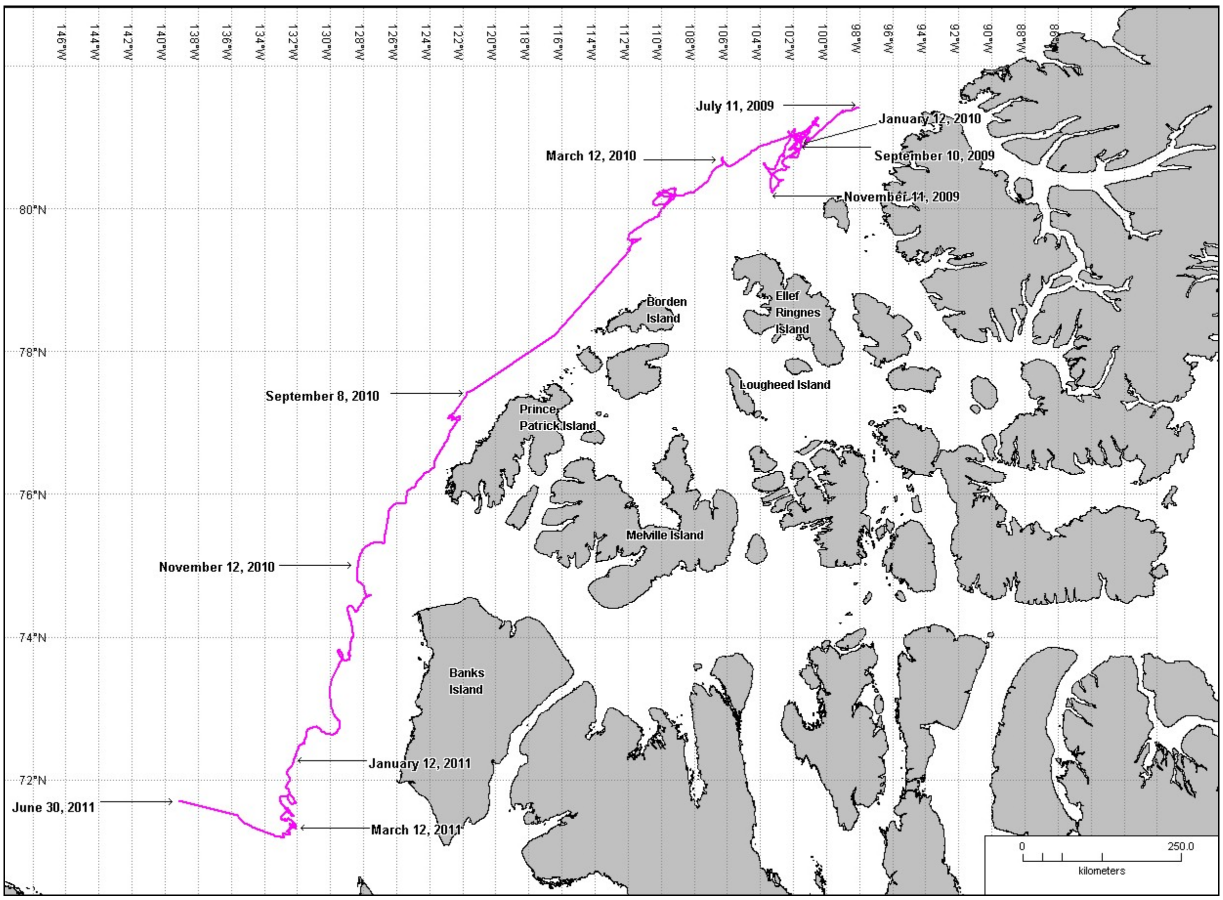

Figure 8-2: Drift of Target 7E from July 11, 2009 to June 30, 2011.

8.1.2 Target 2E

Figure 8-3 shows the trajectory of Target 2E (an Argos beacon with 250 m accuracy) from May 19, 2009 to June 30, 2011, from approximately 80.5° N to 75.8° N. However, Target 2E left the region of interest on August 14, 2010 as it entered the islands of the Canadian Arctic Archipelago at approximately 79.3° N, hence the drift speed and direction analyses for this target extend only to August 13, 2010. At times, the target displayed a very erratic drift pattern, as indicated in the figure below, and we believe this erratic pattern is due to problems with the beacon electronics, as the small random excursions are a few km, which is considerably larger than the expected error for a properly functioning beacon (+/- 250 m--similar to errors seen on June 18th for example). The beacon does at times appear to drift in a reasonable manner. The total distance traveled between May 2009 and mid-August 2010 is 1248.2 km (based on the approximately 24-hourly re-sampled data), with net distance covered of 158.3 km. The mean drift speed for the May 2009-mid-August 2010 period is 2.9 km/day, and the median drift speed is 1.4 km/day. Drift speeds are not very variable throughout the time period, with a standard deviation of 3.6 km/day. Drift statistics for Target 2E are summarized in Table 8-1.

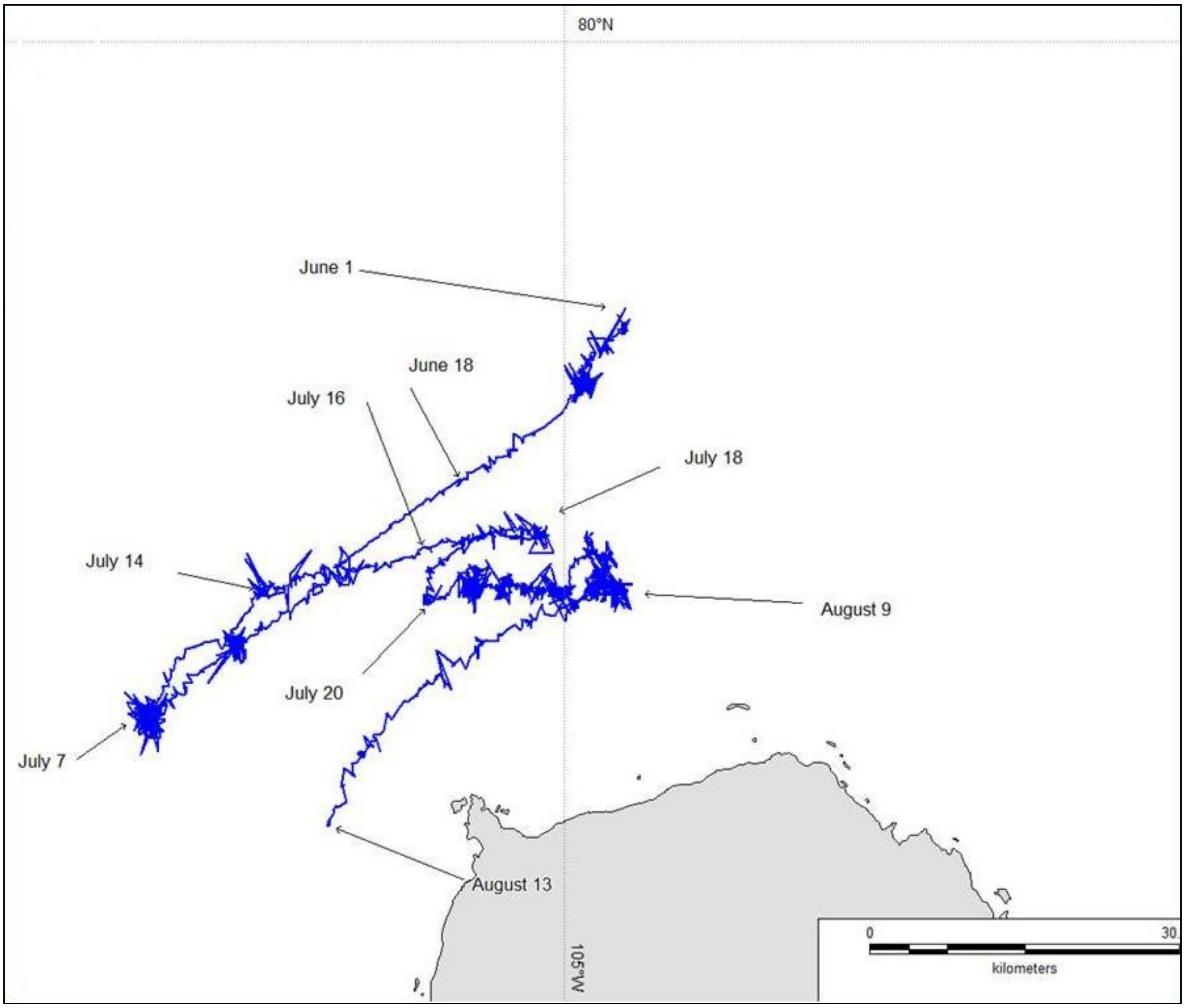

Figure 8-3: Drift of Target 2E from May 19, 2009 to June 30, 2011.

8.1.3 Target 2PP

Figure 8-4 shows the path of Target 2PP (an Argos beacon with 250 m accuracy) from July 29, 2009 to August 22, 2010, over which period it moved from approximately 77° N to 76.9° N. The target remains in the same region near the north coast of Prince Patrick Island throughout the whole period, drifting a total distance of 187.6 km, but only a net distance of 13.3 km. The target drifted almost continuously, remaining stationary only 2% of the time. The mean drift speed for late July 2009-August 2010 is 0.5 km/day, and the median drift speed is 0.3 km/day (the median of all non-zero speeds is 0.3 km/day, and the mean is 0.6 km/day). Drift speeds show a standard deviation of 1.0 km/day. Drift statistics for Target 2PP are summarized in Table 8-1

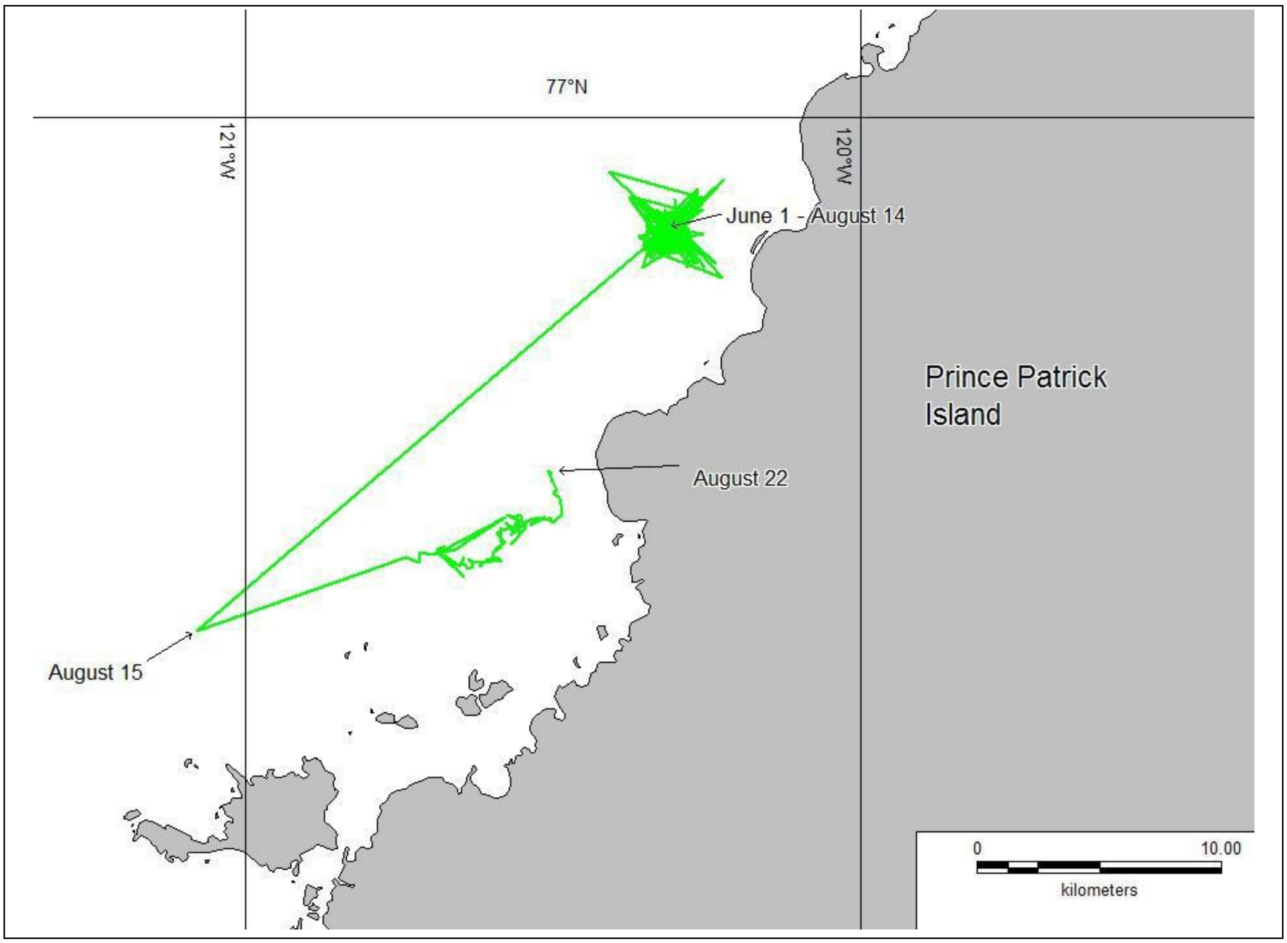

Figure 8-4: Drift of Target 2PP from July 29, 2009 to August, 22, 2010.

8.1.4 Target 1ER

Figure 8-5 displays the trajectory of Target 1ER (an Argos beacon with 250 m accuracy) from April 19, 2010 to June 13, 2011, over which time it drifted from approximately 79.7° N to 74.3° N. However, Target 1ER left the region of interest on August 14, 2010 as it entered the islands of the Canadian Arctic Archipelago at approximately 78.9° N, hence all drift speed and direction analyses for this target extend only through August 13, 2010. The target tends to alternate its drift direction between the southwest and northeast until it begins drifting nearly due south into the Archipelago. Target 1ER drifts toward the southwest for 27% of the study period, and to the northeast for 37% of the time. The total drift distance between mid-April and mid-August 2010 is 433.1 km, with a net drift of 89.5 km. The mean drift speed for the period of interest is 4.1 km/day, and the median is 2.1 km/day. Drift speeds prove somewhat variable, with a standard deviation of 4.9 km/day. Drift statistics for Target 1ER are summarized in Table 8-1

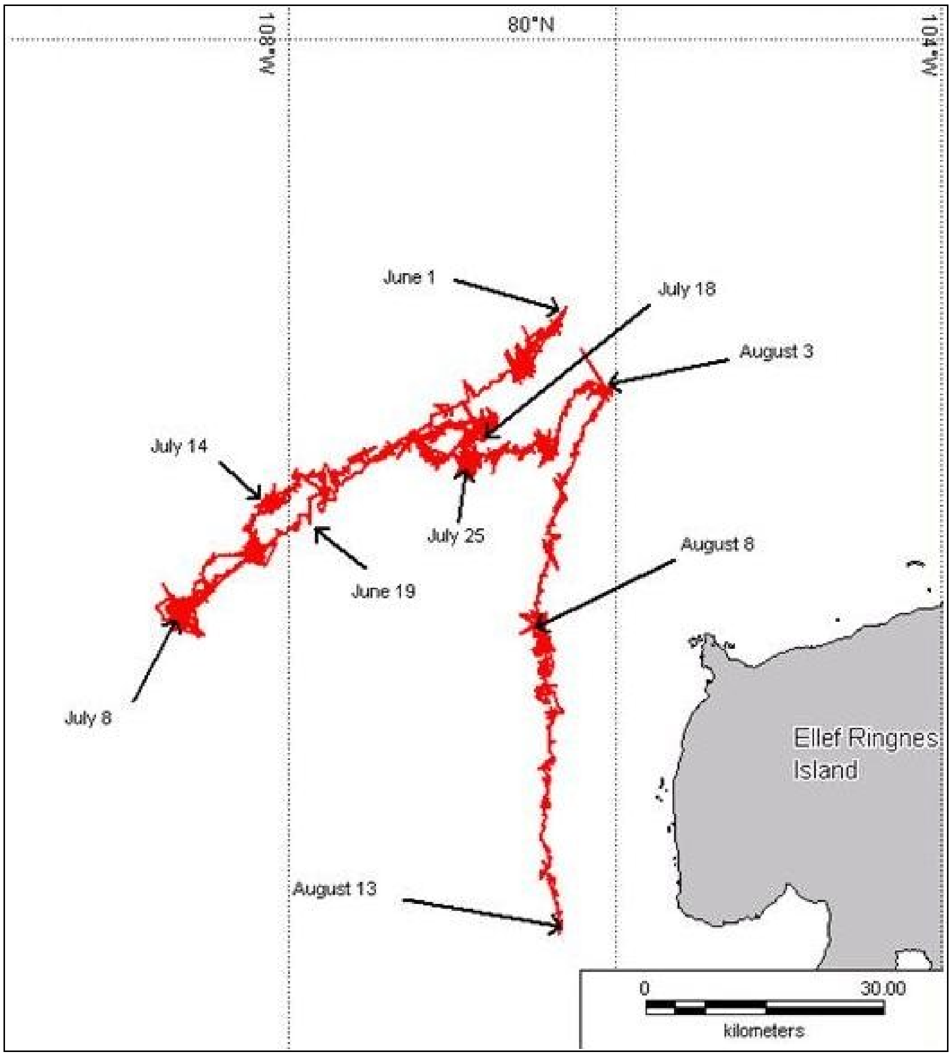

Figure 8-5: Drift of Target 1ER from April 19, 2009 to June 30, 2011.

8.1.5 Target 1B

Figure 8-6 shows the path of Target 1B (an Iridium beacon with 2.5 m accuracy) from April 11 to November 17, 2010, from approximately 78.2° N to 76.1° N. The drift is generally toward the southwest throughout the period of interest, as the target drifts along the western margin of the Archipelago.

However, the target drifts toward the southwest for only 42% of the study period, which indicates that the most rapid drift took place in this direction. Target 1B is never stationary during this time period, and drifts a total of 419.8 km over a net distance of 319.5 km. The mean drift speed is 2.0 km/day, and the median speed is 0.01 km/day. Drift speeds remain under 1.0 km/day until about mid-August, at which time the target begins a faster overall drift more on the order of 5 km/day until early October. From then until October 22, drift speeds again fall below 0.5 km/day and remain this low throughout this short period. From October 22 to November 17, drift speeds are again on the order of 8-10 km/day. Drift speeds vary somewhat, registering a standard deviation of only 4.0 km/day. The target's overall drift pattern indicates a current down the western margin of the Archipelago that is fairly constant in direction and intensity, with the target straying from this current pattern only when forced into inertial oscillations during late August, and when caught in a largely wind-driven drift pattern from September 18 through late October. Drift statistics for Target 1B are summarized in Table 8-1.

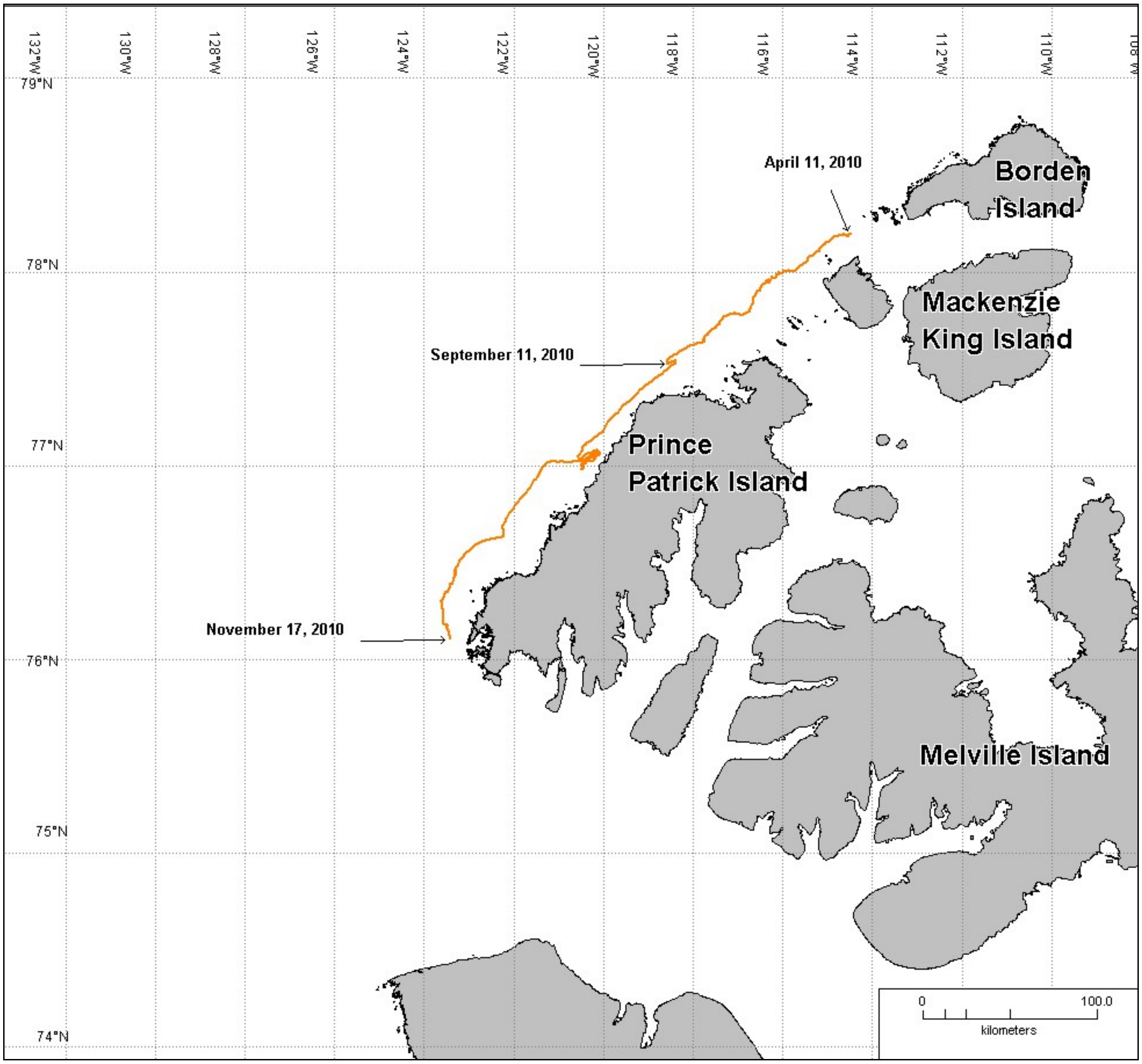

Figure 8-6: Drift of Target 2PP from April 11, 2010 to November 17, 2010.

8.2 Drift Speed Analysis

The drift speed analysis was done following the guidelines of the previous project progress report. A set of three graphs are presented for each beacon:

1) Drift speed distribution. This graph is a vector representation of the ice drift speeds and directions. The distribution of this graph gives the preferential direction and the perturbations of the trajectories.

2) Frequency of the drift speed distribution. This graph gives the cumulative occurrences of each ice drift direction. This can help to clarify the preferred ice drift direction when the distribution tends to be uniform.

3) Exceedance probability of the drift speed. This graph presents the probability that an ice drift speed value can be exceeded. For instance, the 0 km/day speed value can be exceeded 100% of the time or there is 100% probability that any magnitude of the ice drift vector will be greater than 0 km/day. When the distribution of the data is so asymmetric that the mean value and the median are not close values, then the median is a better estimator since the mean value can be affected for only one value greater than one order of magnitude.

8.2.1 Target 7E

Figure 8-7 shows the magnitude and distribution per direction of Target 7E speed in km/day. The target drifted mostly toward the south-southwest from July 2009 to June 2011, and generally at its highest speeds in this direction. The target drifted most often toward the southwest and south-southwest (see Figure 8-8).

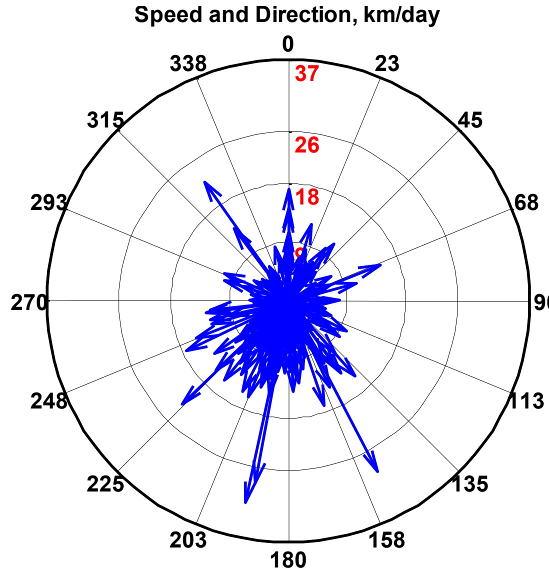

Figure 8-7: Drift speeds and associated azimuthal directions of Target 7E (red number) for the period July 11, 2009-June 30, 2011.

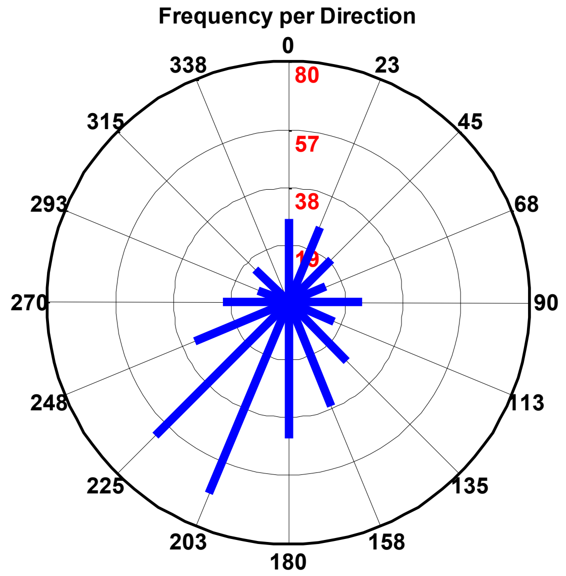

Figure 8-8: Frequency of the drift per azimuthal direction (red number) for Target 7E for the period July 11, 2009-June 30, 2011.

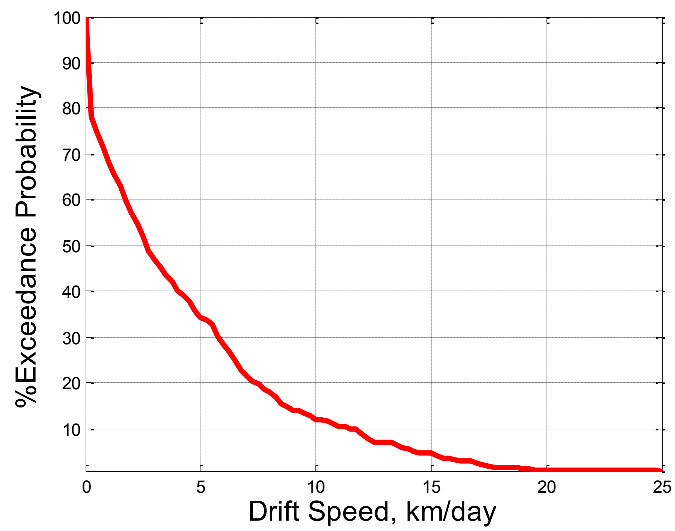

Figure 8-9: Exceedance probability of the drift speeds for Target 7E for the period July 11, 2009-June 30, 2011.

8.2.2 Target 2E

Figure 8-10 the magnitude and distribution per direction of Target 2E speed in km/day. Target 2E drifted in nearly all directions between May 2009 and August 2010, with its highest speeds most often reached as it drifted toward the southwest. The target most frequently drifts toward the south-southwest (see Figure 8-11).

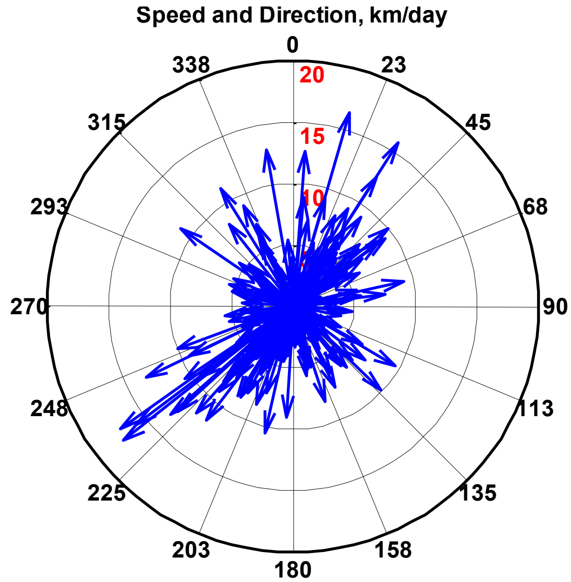

Figure 8-10: Drift speeds and associated azimuthal directions for Target 2E (red number) for the period May 19, 2009-August 13, 2010.

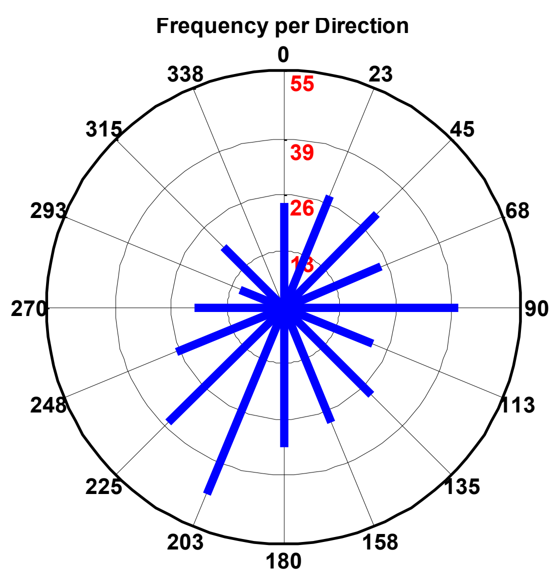

Figure 8-11: Frequency of the drift per azimuthal direction (red number) for the Target 2E for the period May 19, 2009-August 13, 2010.

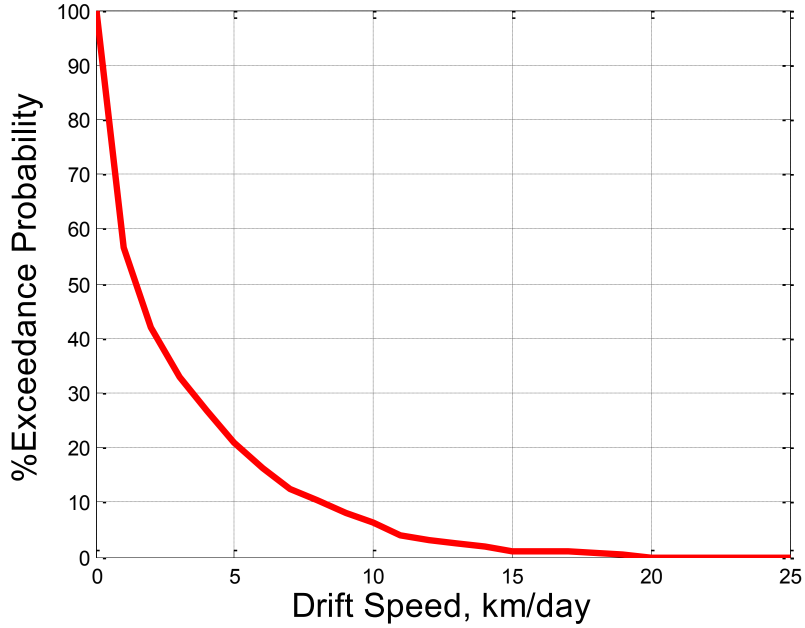

Figure 8-12: Exceedance probability of the drift speeds for the Target 2E for the period May 19, 2009-August 13, 2010.

8.2.3 Target 1E

Target 1E left the region of interest after remaining stationary for a period of time. It drifted south to enter the Archipelago, and so out of the region of interest. Therefore, no drift speed and direction or exceedence probability plots were made for this beacon.

8.2.4 Target 2PP

Figure 8-13 shows the magnitude and distribution per direction of Target 2PP speed in km/day. Drift occurs in nearly all directions from July 2009 to August 2010, with the fastest speeds occurring toward the southeast and east-northeast. Drift throughout the period occurs about evenly in all the cardinal directions, however an eastward drift was noticeably quite frequent (see Figure 8-14).

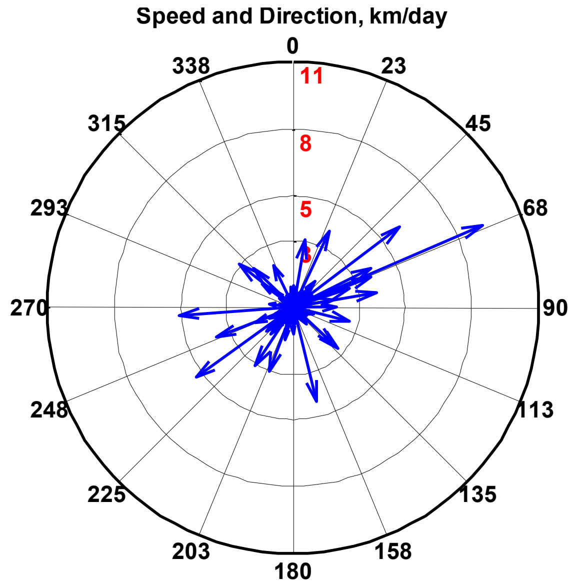

Figure 8-13: Drift speeds and associated azimuthal directions of Target 2PP (red number) for the period July 29, 2009 to August 22, 2010.

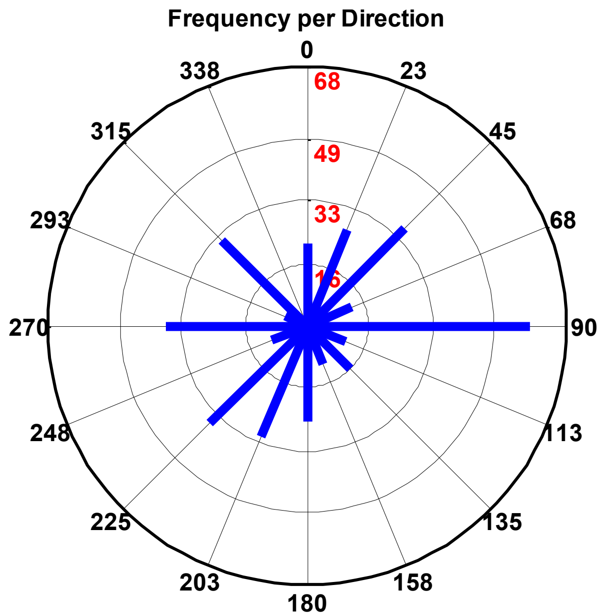

Figure 8-14: Frequency of the drift per azimuthal direction for Target 2PP (red number) for the period July 29, 2009 to August 22, 2010.

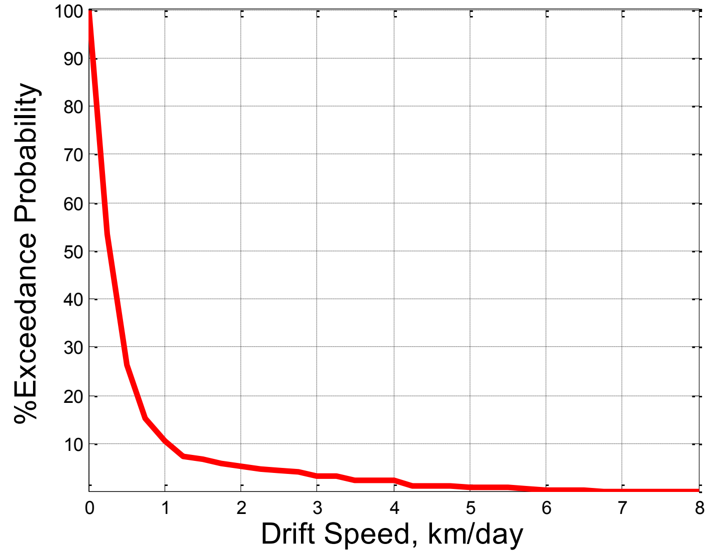

Figure 8-15: Exceedance probability of the drift speeds for Target 2PP for the period July 29, 2009 to August 22, 2010.

8.2.5 Target 1ER

Figure 8-16 shows the magnitude and distribution per direction of Target 1ER speed in km/day. The target drifts erratically in all directions between April and August 2010, but most frequently drifted toward the south, southwest, and east-northeast (see Figure 8-17).

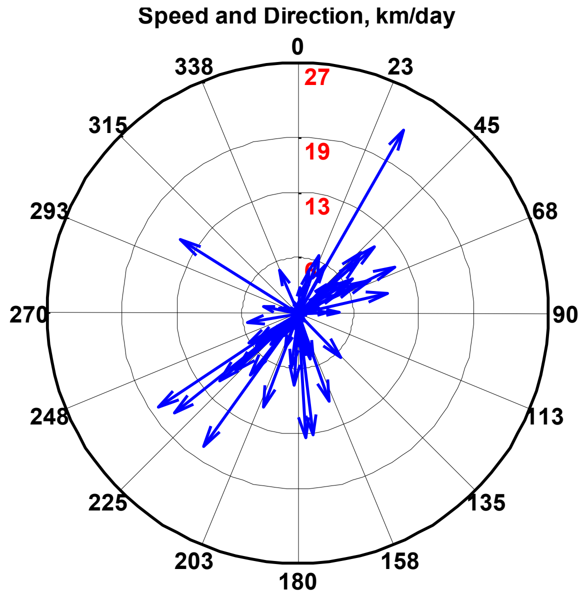

Figure 8-16: Drift speeds and associated azimuthal directions of Target 1ER (red number) for the period from April 19 to August 13, 2010.

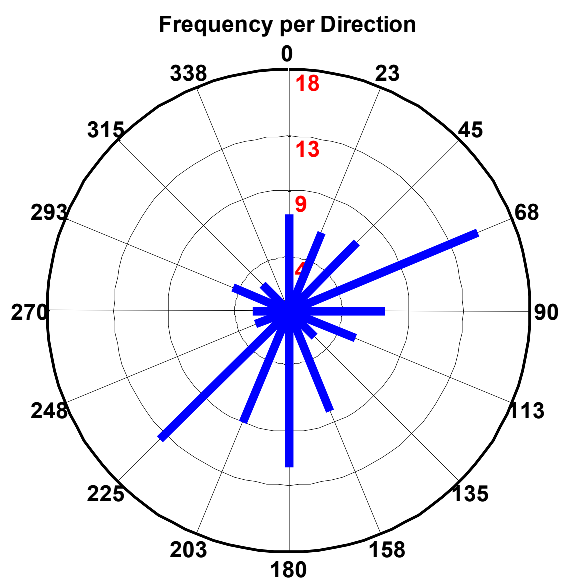

Figure 8-17: Frequency of the drift per azimuthal direction for Target 1ER (red number) for the period from April 19 to August 13, 2010.

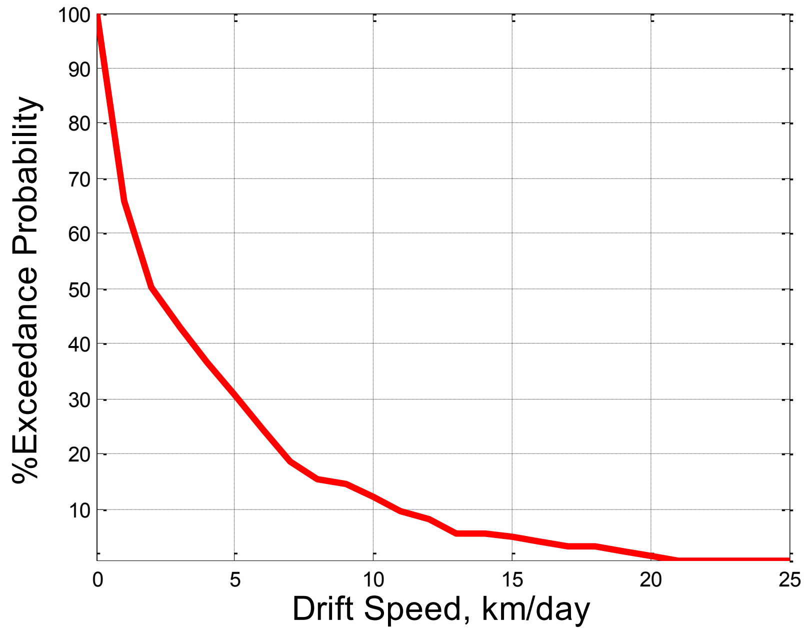

Figure 8-18: Exceedance probability of the drift speeds for Target 1ER for the period from April 19 to August 13, 2010.

8.2.6 Target 1B

Figure 8-19 shows the magnitude and distribution per direction of Target 1B speed in km/day. From April to November 2010, the target drifts mainly toward the south and southwest (see also Figure 8-20), and moves fastest when drifting to the southwest.

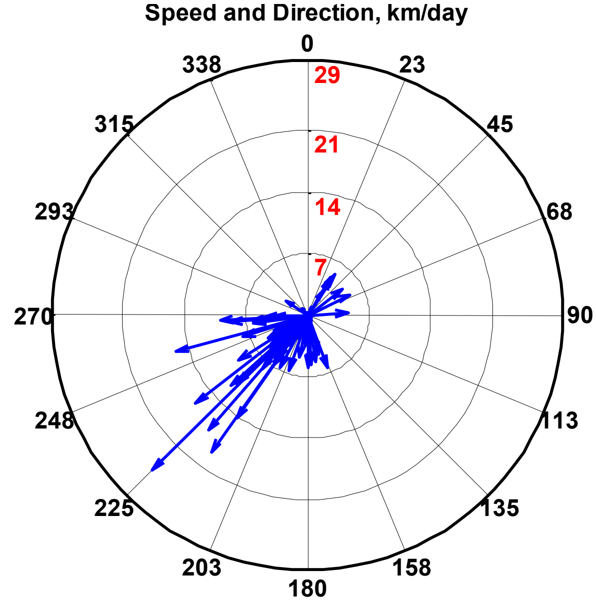

Figure 8-19: Drift speeds and associated azimuthal directions of Target 1B (red number) for the period from April 11 to November 17, 2010.

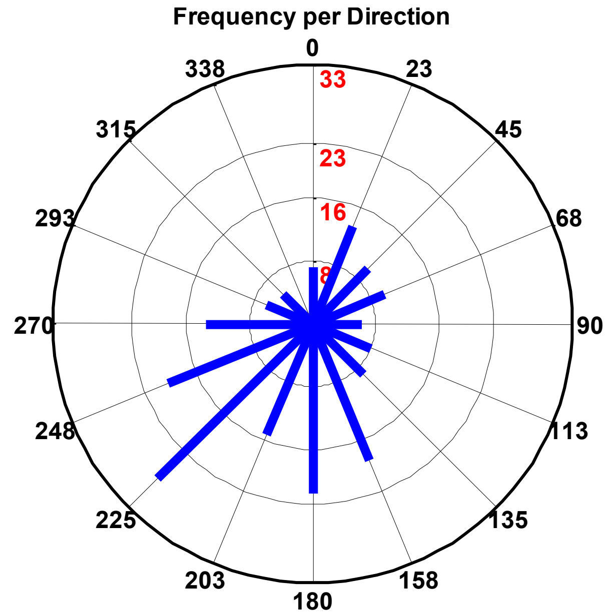

Figure 8-20: Frequency of the drift per azimuthal direction for Target 1B (red number) for the period from April 11 to November 17, 2010.

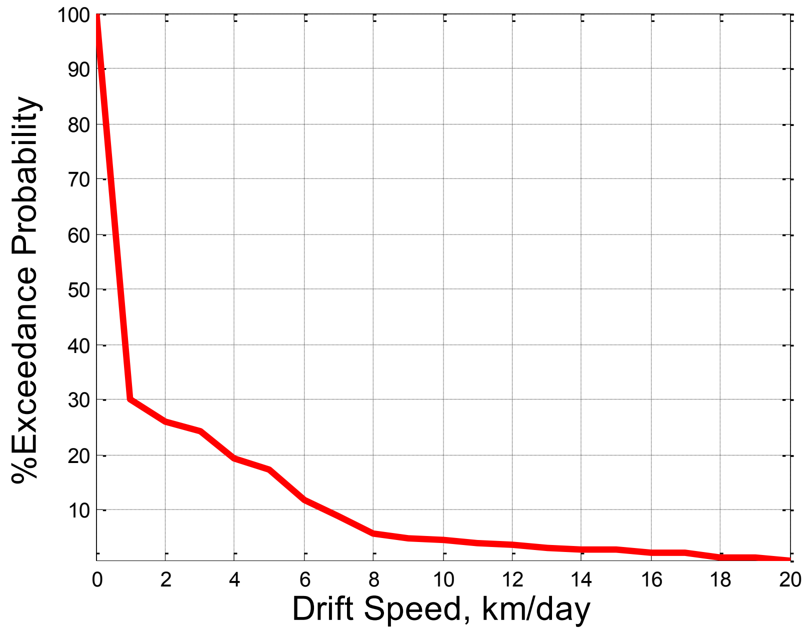

Figure 8-21: Exceedance probability of the drift speeds for Target 1B for the period from April 11 to November 17, 2010.

8.3 Drift Review

All six targets show an overall drift toward the southwest while outside the margin of the Archipelago, but Targets 1E, 1ER, and 2E end up drifting almost due south into the Archipelago (see Table 8-1 for drift statistics).

Table 8-1: Drift statistics and type of satellite used for all targets, May 19, 2009 to June 30, 2011.

Target	Mean Drift Speed (km/day)	Median Drift Speed (km/day)	Drift Speed St. Dev (km/day)	Total Drift Distance (km)	Net Drift Distance (km)	% of Time Period Spent Drifting in Non-SW Direction	Satellite Type
7E	4.4	2.7	5.1	2142.2	1452.9	57%	Iridium
2E	2.9	1.4	3.6	1248.2	158.3	N/A	Argos
2PP	0.5	0.3	1.0	187.6	13.3	N/A	Argos
1ER	4.1	2.1	4.9	433.1	89.5	73%	Argos
1B	2.0	0.01	4.0	419.8	319.5	58%	Iridium

Targets 7E, 1B, and 2PP drift along the western margin of the Archipelago for their beacons' entire transmission records. Target 7E eventually turns toward the west-northwest as it reaches the southern coast of the Beaufort Sea, and continues roughly parallel to the shoreline. The drift of all targets is consistent with the flow of the Beaufort Gyre toward the southwest along the Archipelago's western margin, with the exception that three of the targets drift south into the Archipelago. In an earlier report, we obtained wind data from NCAR to show that most of the observed beacon motion was due to wind. We could continue this work for other beacons if the clients so desired, but it is not within the scope of the current project. However, given the fact that the drift of all the targets between about 79° N and 81° N is more erratic in direction compared to the much more uniformly southwest drift at lower latitudes along the Archipelago's western margin, it seems the targets at the most northern latitudes were too far east to be entrained in the main part of eastern branch of the Beaufort Gyre.

The mean drift speed of Target 7E is slightly higher than that for Target 1B, which is not surprising given its location farther offshore, in deeper (>200 m depth) water where currents tend to be faster, and/or the coastal boundary effects are not as significant. Also, Targets 7E, 1B, and 2PP all appear to get caught up in a looping drift pattern around 77 N, which was likely due to a widespread wind event, rather than a near-shore tidal event, given the fact that Target 7E displays this looping behavior more than 50 km offshore.

The number of available Ice Island targets decreases as they move south due to features moving into the islands, features breaking up, or beacons failing, so that in the extreme southern Beaufort Sea, only Target 7E remains. The beacon on Target 2PP died on August 22, 2010. This feature stayed around Prince Patrick Island during the period that the beacon operated. Once this feature broke or breaks free from this area, it could travel south into the southern Beaufort Sea, however, it was considered to be a multi-year hummock field, and so would be more likely to break up than Ice Island 7E. Target 7E, the largest of the targets, was the only target to have reached the lease areas of the southern Beaufort Sea with a functioning beacon, and it took nearly two full years to do so while decreasing by about 40% in size.

9 OVERALL PROJECT SUMMARY – SIZE & SHAPE ANALYSIS

9.1 Changes in Size

Size analysis is governed by the availability of imagery. Table 9-1shows the size changes of each target over the two year project period. The records for targets 1E and 2E are short in comparison with 7E because these two targets drifted south from Ellef Ringnes Island into the Queen Elizabeth Islands in August 2010, exiting the area of interest. Consequently no other images were collected after their exit.

Table 9-1: Time Series summarization of Area Changes for Targets 1E, 2E, and 7E.

Image Acquisition Date (DD-MM-YY)	Target	Area (km^2)	Area Change (km^2)	% Change from Previous
25-Aug-09	1E	9.49		
31-Oct-09	1E	9.80	0.31	3.27
22-May-10	1E	7.03	-2.77	-28.27
		Change from Initial	**-2.46**	
		cumulative % change from initial		-25.92
31-Aug-09	2E	7.90		
28-Oct-09	2E	7.22	-0.68	-8.61
26-May-10	2E	6.66	-0.56	-7.76
		Change from Initial	**-1.24**	
		cumulative % change from initial		-15.70
27-Aug-09	7E	19.15		
29-Oct-09	7E	15.95	-3.20	-16.71
17-Apr-10	7E	14.65	-1.30	-8.15
15-Jun-10	7E	13.87	-0.78	-5.32
18-Jul-10	7E	12.88	-0.99	-7.14
12-Sep-10	7E	11.85	-1.03	-8.00
11-Apr-11	7E	11.74	-0.11	-0.93
15-May-11	7E	11.63	-0.11	-0.94
		Change from Initial	**-7.52**	
		cumulative % change from initial		-47.18
		Average Total Area Change	**-3.74**	
		Average total % change		**-29.60**

Although the data set in Table 9-1 is short, some possible patterns can be discerned. Each of the targets has lost significant area over the entire analysis record, with the largest rates of loss occurring in the first year since their initial break up. Specifically Target 7E underwent rapid area losses at the beginning of the record (August 2009 to October 2009), which was then followed by a steady rate of decline over the next 10 months until August 2010. This is further shown by the blue curves Figure 9-1 and Figure 9-2. Although area losses continued throughout the duration of the record, the rate of decay appeared to not only slow, but began to stabilize. This perhaps suggests that once a threshold size (11.85 km2 in the case of 7E) of an ice island is met, the rate and amount of decay and disintegration processes dramatically reduces to a stabilized level. 7E has become a quite rounded feature, which presumably reduces the chances of further break offs.

The above temporal trend and pattern is shown below in Figure 9-1 and Figure 9-2. From August 2009 to September 2010, the feature showed a rapid decrease in size. Relatively little decrease has occurred since then to the end of the recording period, which could in fact be measurement error.

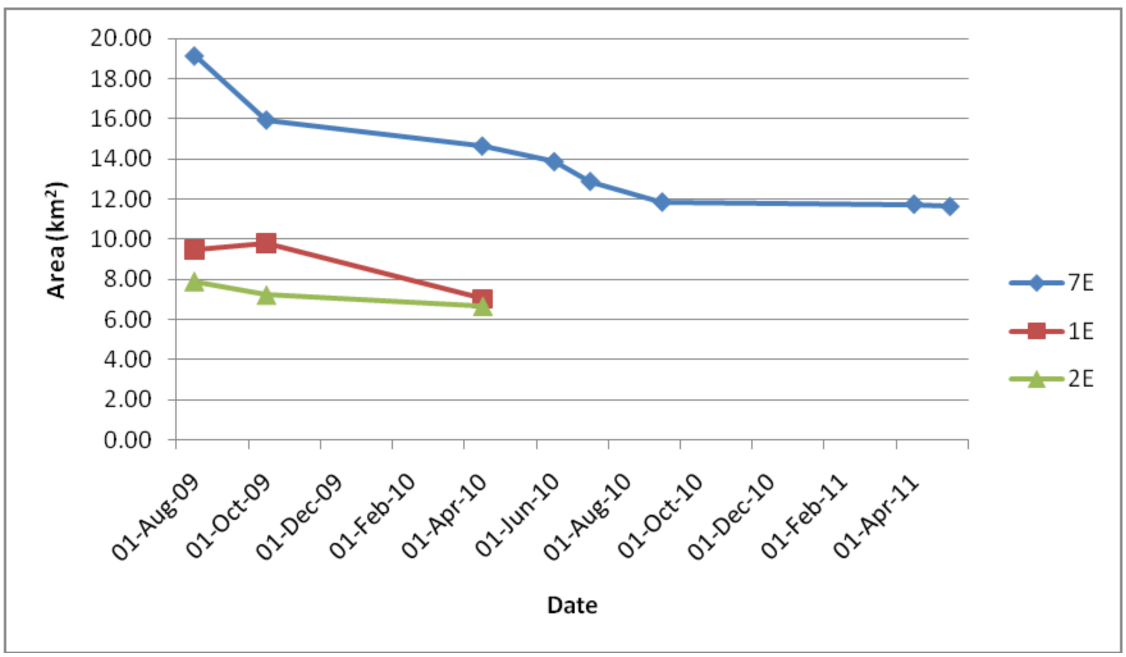

Figure 9-1: Area Changes from August 2009 through May 2011.

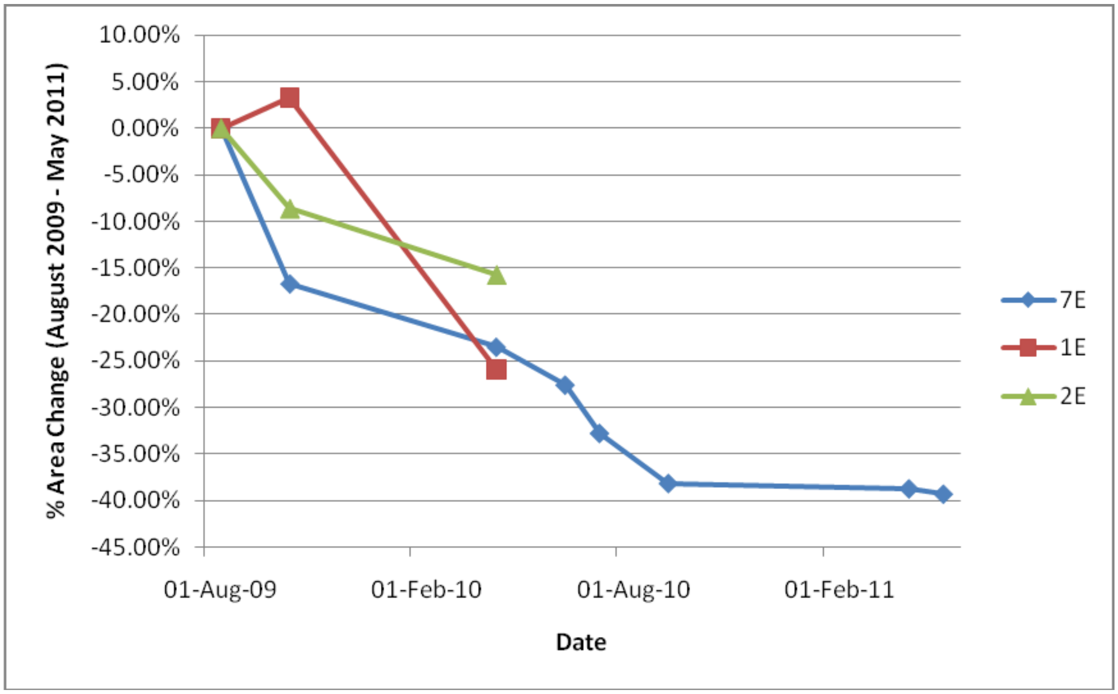

Figure 9-2: Percent Area Changes from August 2009 through May 2011.

The emerging decay pattern described above is investigated further in the following section. The temporal trend observed may additionally be explained as a function of location. This provides a more robust justification to this interesting and important finding.

9.2 Area Changes by Location

It is useful to plot size changes of the principal targeted feature not just against time, but according to the geographic area in which the feature is located. This is done in Figure 9-3. We have divided the coastal drift zone into 8 segments, as shown in Figure 9-3, and the list below, to describe our corridor.

- Ellesmere
- Axel Heiberg
- Ellef Ringnes
- Borden and Brock
- Prince Patrick
- M'Clure Strait
- Banks Island
- Beaufort Sea

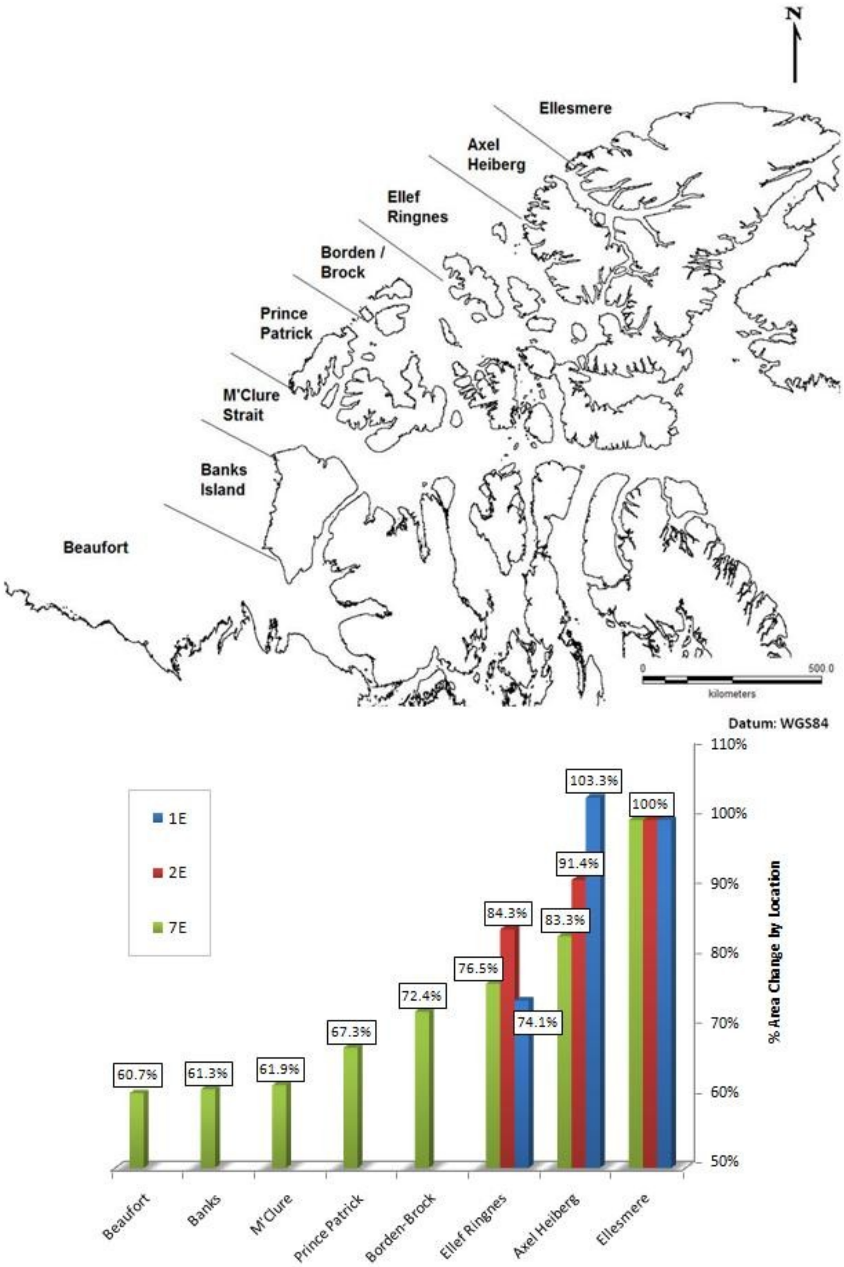

Figure 9-3: Area changes as a function of location from August 2009 through May 2011.

When focusing on Target 7E (green bars), this analysis shows that the pattern and frequency of disintegration exhibits a distinct change as a function location as the target drifts throughout each zone. The rates of decline appeared to follow a negative linear trend between Axel Heiberg Island and the M'Clure Strait ranging from about -5 to -7 % throughout each zone. While in the M'Clure, Banks, and Beaufort zones, the rates of decline dramatically shift to a much more constant and stable regime. This was largely unexpected. The steady, steeper declines observed for the first two thirds of the record nearly became zero. Perhaps Figure 9-3 is showing a relationship between target size and the rate of areal decay of an ice island with its drift location. For the first two thirds of the record Target 7E largely drifted along the coastal region of the High Arctic Islands. It hugged the shallower coastal regimes of Axel Heiberg, Ellef Ringnes, Borden/Brock, and Prince Patrick Islands when compared to the deep water regions of M'Clure, Banks Island, and the Beaufort Sea as it migrated away from the coastline. This finding suggests that the interaction of an ice island drifting through leads and amongst pack ice combined with its drift through areas of convergence created by the fast ice boundary and a compact ice edge enables greater rates of decay when compared with drift away from the coast in deeper water. The more northerly coastal regions would provide a tortuous confined environment for the target so that when it drifts throughout this region, the feature would undergo increased external pressures by the surrounding micro environment leading to increased dynamic processes, such as increased mass / area losses. A smoother unobstructed path in deeper water provides a different set of dynamics, placing less lateral stress on the target.

Generally, there appears to be a direct relationship between target size, the frequency of target decay (rates of decrease), drift duration, and location. Another explanation claimed in section 8.1 for these findings is that once a threshold size is met for drifting ice islands, decay rates and frequency declines on account of the structural integrity of the feature. In either case, the observations made in this general overview were quite unexpected.

9.3 Shift in Area Balance by Feature

We also need to consider area changes of all the fragments that have come from the original feature itself, until they become so small they are no longer considered hazards. We consider a size of 200 m for fragments as the lower limit at which they will not represent a serious hazard for offshore petroleum activities in the Beaufort Sea. For Ice Island fragments, this would refer to the long dimension, as they tend to be rectangles; for MYHFs, this would refer to an approximate diameter or a long axis depending on the shape.

For Target 7E from April 2010 through May 2011, we were able to track 5 fragments surrounding Target 7E between images (see Figure 9-4). The observed trend for the fragments is to lose area over time in a similar pattern. Irrespective of the size of the fragment, the fragment appears to have accelerated area losses over the spring and summer period (April – September), then begins to slow down over winter, followed by an increase in area loss in the spring as shown in Figure 9-4. This suggests similar environmental factors i.e. weather, drift, surrounding sea ice; all contribute to the area loss pattern observed, since the same overlying environmental conditions would be present during the respective season.

Figure 9-4: Percent Area Change of Fragments around 7E from April 2010 – May 2011.

9.4 Changes in Shape

Figure 9-5 through Figure 9-7 below provide overlay image sequences of targets 1E, 2E and 7E respectively. Specifically the overlays address changes in shape of each target. This is facilitated by analyzing the change in shape from the first image to the final image collected.

Target 1E and 2E generally maintained their shapes for both of their records. The edges of the features became sharper, with the major changes in terms of area loss occurring to the extremities of the targets. The targets decayed along rib lines forming long shard type fragments, with fragments also breaking off into blocky pieces. The record is unfortunately not long enough in time for either of these targets to show a trend or pattern in shape change; however break up did occur along rib lines that were exposed to the surrounding environment on the periphery of the target. This suggests that wave, and ocean processes are acting as important external environmental parameters on each of targets as the drift along the coastline of the Canadian High Arctic Islands.

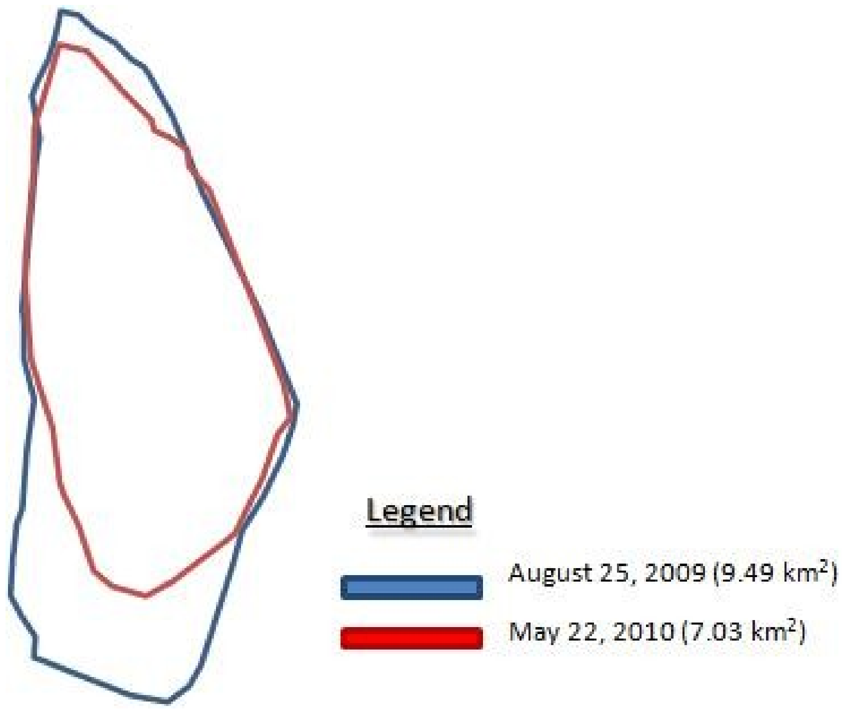

Figure 9-5: Overlay for Target 1E Imagery from August 25, 2009 (blue) through May 22, 2010 (red).

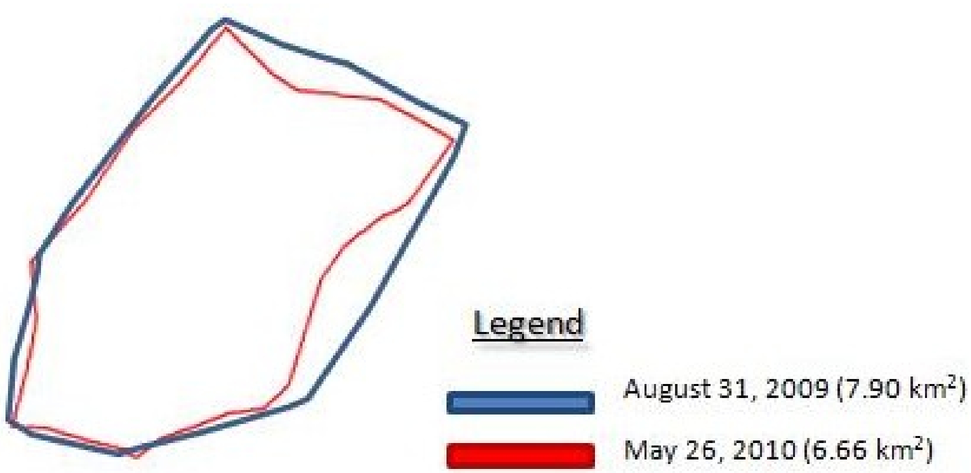

Figure 9-6: Overlay for Target 2E Imagery from August 31, 2009 (blue) through May 26, 2010 (red).

Target 7E has undergone significant changes in terms of both area change, and shape alteration over the course of our analysis period when compared with Targets 1E and 2E. Since drift had commenced from Northern Ellesmere Island, the distinct angular edges and jagged corners have largely become rounded.

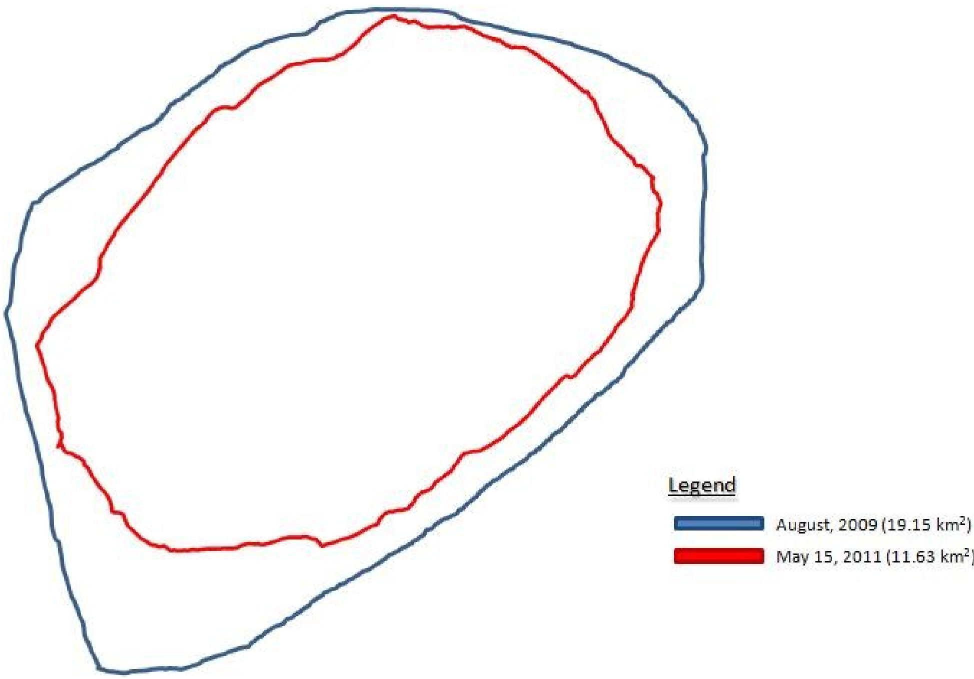

Figure 9-7: Overlay for Target 7E Imagery from August 27, 2009 (blue) through May 15 (red) 2011.

10 CONCLUSIONS AND RECOMMENDATIONS

In this section we summarize all the key findings that relate to understanding and managing the hazards posed by Ice Islands and MYHFs to offshore petroleum operations in the southern Beaufort Sea. In all cases, the data available are extremely few and far too small to draw any final conclusions. However, in the absence of any other data, they are exceptionally important to begin to set critical design and operations parameters.

10.1 Data

10.1.1 Arrivals in AOI

Hazardous Ice Islands can definitely arrive in the Alert Zone updrift of the AOI. The project measured one instance, which was the single feature tracked into the zone. It is therefore expected that hazardous Ice Islands can transit through the AOI.

No MYHF transits through the AOI were observed in this project. However, from other data it is known that they can travel through the AOI.

10.1.2 Size

The one II we measured coming into the alert zone of the AOI was 12 km^2. This is probably representative of a large II that could transit the AOI.

From other data, we could estimate that a large MYHF transiting the AOI might be 6 km^2

10.1.3 Shape

IIs that arrive in the AOI tend to be oval, with a fairly smooth outline and no jagged protrusions. This shape is presumably a stable shape.

For MYHFs, other data suggest an interchange between shapes over time. They usually calve as angular features, then become rounded as they drift (past Banks Island into the Beaufort), then switch back to more angular features (moving out of the Canadian Beaufort towards Alaska), as they thin from melting.

10.1.4 Velocity

Peak velocity of Ice Islands in the AOI was measured at 35.1 km/day (0.4 m/sec). This is probably fairly close to a maximum that could be expected for any II.

Peak velocity of MYHFs was measured at 27.7 km/day (0.3 m/sec), but not in the AOI. It is likely that a larger data set would show the velocities of both types of features to be fairly similar.

10.1.5 Transit time

Travel time of Ice Islands from calving to the AOI is approximately 2 years, but might be as low as 0.9 or as high as 3.5 years.

Travel time of MHYFs from a breakout zone at the central part of Prince Patrick Island to the AOI is estimated at about 0.7 years, and could be as low as 0.5 years or has high as just over a year.

10.1.6 Reduction of Number of Arrivals

Many Ice Islands are diverted into the channels of the Archipelago where they no longer present hazards to Beaufort Sea offshore operations, or ground on the shallows of the north shore of the Archipelago. Our project indicated that only about 1/5 of Ice Islands that calve from the Ellesmere region reach the AOI.

We have no measurements for MYHFs. Since they are produced farther south, it is likely that a higher proportion reaches the AOI.

10.1.7 Decay of Size of Main Feature

From the data at hand, we can state a first estimate that Ice Islands arriving into the AIO will be 40 % smaller than when they calved.

For MYHFs, we have no direct data, but, assuming they have the same structural integrity and thermal mass as Ice Islands, they will undergo much less degradation, perhaps only 5% for ones originating off Brock Island and 7% for ones originating off Prince Patrick Island, so they will arrive in the AOI substantially the same size as when they broke off.

10.1.8 Change in Nature of Hazard

As Ice Islands decay, the main original feature becomes smaller and is surrounded by a field of fragments. These fragments decay over time, creating more numerous and smaller fragments. In some cases there were up to 33 fragments within a radius of 5 km, while in other cases 8 fragments in a radius of 10 km representing 33% of the area of the original feature. Fragments below the hazard limit (200m) seem to decay extremely rapidly to much smaller sizes.

10.2 Hazard Management

10.2.1 Probability of impact

We do not have enough data to calculate even a first reasonable estimate of this critical parameter.

10.2.2 Impact Force

We have enough data on velocity, shape, size and mass of both Ice Islands and MYHFs to calculate reasonable first guesses of this critical parameter, for the types of structures expected to be put in place, but not enough data to design such structures.

10.2.3 Setting Alert Zone

There are enough data on velocity and ability to forecast drift, as well as on feature draft and area, and our capability to spot smaller hazardous features, to design the first draft of alert zones and procedures.

10.2.4 Forecasting Size upon Arrival

It would be useful to be able to predict the amounts of fracturing that an II or MYHF will undergo when well updrift of the AOI. This would help us estimate the size of the feature and the number of fragments around it when it might come into the alert zone. This is not yet possible.

10.2.5 Spotting Hazardous features

RadarSat imagery is an essential tool for this kind of research project. It works very well to depict fine detail of ice features. However, it is very expensive to plan and analyze, especially on moving targets when the footprint is so small and there are significant time lags between ordering and acquiring. Imagery is best combined with beacon tracks for research and hazard management on these features.

It would be useful to know more about the spatial relation of fragment clusters to the main feature, as the main feature, being much larger, is easier to spot by satellite imagery. If there were regularities in cluster positioning relative to the main feature, this could be used as a technique for hazard management. To date, we have not found any such regularities.

10.2.6 Tracking Hazardous Features

Beacons are critical technologies for long and short term tracking of hazardous features. However, this is a hostile environment for drift beacons; their performance is quite erratic in meeting the challenges. Sometimes they fail immediately and totally; other times, they function intermittently; other times, they work well up to their design lifespan. There are no means with these beacons of verifying why they failed – electronic problems, battery discharge, change of orientation losing sky visibility, sinking in a melt puddle or polar bear attack.

10.3 Recommendations

This project is the first of its kind. It is showing where more research is required, on a variety of issues.

10.3.1 Image Acquisition Planning and Execution

CIS has proven to be an invaluable partner in supplying imagery. Donation of images for this project by CIS was the only way the project could have gone ahead. Depending on donated images however, has limitations, as supporting this kind of project is not CIS' primary mandate. In order to get high resolution images of moving targets, the only feasible solution is to pay for the short turn-around order.

10.3.2 Genesis of Hazardous Features

Predicting the calving of individual ice islands is not important as the transit time is so long and the events are easy to spot. However, it would be useful to have better understanding of the environmental forces driving calving so it could be predicted how much more ice might calve, when and what the largest size of islands might be, over the next 40 years, which could be the lifespan of a fixed production platform. The project has not attempted to measure this aspect, but has found evidence suggesting some particular dynamics that could be tested.

Prediction of breakout of MYHFs is not possible at this time and there seems to be no research on this. Our project found features that seemed to be incipient MYHFs but in 1 case it did not break out and in another, we lost the beacon before the feature could be imaged. It would be important to track the growth and decay of the shear zone ice off places like Prince Patrick Island to advance our understanding of this phenomenon.

10.3.3 Forecasting Short Term Drift

The dimensions of the alert zone and procedures need to be significantly improved, with better short term ice drift forecasting techniques. Our ability to forecast short term drift of hazardous features is limited to within a radius of about 1 nautical mile over a 24-hour period. This could be improved by up to 10% with about a year of full time research on better forecasting models for the southern Beaufort Sea (which Canatec is working on in-house), and by having the right number of real time meteorological and oceanographic data inputs on forcing parameters. For routine operations, the cost of developing improved forecasting and implementing it with better data streams would be a tiny fraction of the revenue generated by increasing the time on operations.

10.3.4 Forecasting Breakup and Decay

It would be useful to be able to predict somewhat the possible amounts of fracturing that will occur well updrift of the AOI. This would help us estimate the size of the feature and the number of fragments around it when it might come into the alert zone.

10.3.5 Making Better Drift Beacons

Manufacturers of beacons need to continue to improve these instruments. The difficulty in doing so is that the market is very small, so it is hard to finance their development. One suggestion would be for an alliance to be made with major uses like petroleum companies to provide a mechanism for funding such improvements. Since safe operations planning is so important, beacon deployment from aircraft needs to be certified as airworthy and drone techniques need developing.

10.3.6 Gathering More Data

More data are required to get better understanding of:

- Size, shape and thickness of arrivals in the AOI
- Peak velocities of arrivals in the AOI
- Percentage of features that get trapped, diverted or decayed before arriving the AOI
- Patterns of clustering of fragments around the main feature updrift of the AOI.